Remote Effects Modulating the Spin Equilibrium of the Resting State of Cytochrome $P450_{cam}$ – An Investigation Using Active Site Analogues

Martin Lochner, Linjing Mu, Wolf-D. Woggon*

Department of Chemistry, University of Basel, St. Johanns-Ring 19, 4056 Basel, Switzerland
Fax: (+41)-61-267-1102, e-mail: wolf-d.woggon@unibas.ch

Received: January 14, 2003; Accepted: March 20, 2003

Abstract: The crystal structure of the resting state of cytochrome $P450_{cam}$ (CYP101), a heme thiolate protein, shows a cluster of six water molecules in the substrate binding pocket, one of which is coordinating to iron(III) as sixth ligand. The resting state is low-spin and changes to high-spin when substrate camphor binds and H_2O is removed. In contrast to the protein, previously synthesised enzyme models such as $H_2O{-}Fe^{III}(porph)(ArS^-)$ were shown to be purely high-spin. Iron(S^-)porphyrins with different distal sites mimicking proposed remote effects have been prepared and studied by cw-EPR. The results indicate that the low-spin of the resting state of $P450_{cam}$ is due to the fact that the water molecule coordinating to iron has an OH^--like character because of hydrogen bonding and polarisation of the water cluster, respectively.

Keywords: cytochrome P450; enzyme models; EPR spectroscopy; porphyrinoids; spin states

Introduction

After more than 30 years of research P450-catalysed reactions have been recognised as one of nature's most common and sophisticated methods to oxidise endogenous compounds in prokaryotic and eukaryotic cells.[1] Accordingly, P450 s can be isolated from bacteria,[2] plants[3] and different tissues of mammals,[4] where numerous isozymes participate highly specifically in the metabolism of compounds as diverse as steroids, fatty acids and alkaloids. The same reactivity is also common to those P450 s acting on xenobiotics like toxic compounds and drugs and they can be isolated, e.g., from liver microsomes. The membrane-bound hepatic P450 s generally accept a broad spectrum of substrates, which is understood as a method of detoxification in order to render lipophilic compounds water soluble and excretable.

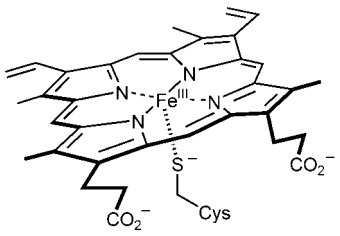

Figure 1. Molecular structure of the P450 active site.

A common feature of the P450 molecular structure is an iron(III) protoporphyrin IX (heme *b*) cofactor in the active site (Figure 1). The fifth proximal cysteinate ligand is provided by the polypeptide chain of the globular protein and is responsible for the unique feature of these enzymes to activate molecular dioxygen towards insertions into C-H bonds.

Among these enzymes, the P450 s responsible for epoxidation of alkenes and the hydroxylation of non-activated C-H bonds (RH), utilising either NADH or NADPH as electron sources (Equation 1), have been studied extensively.[1,2] Experiments with labelled $^{18}O_2$ have shown that one of the oxygen atoms is incorporated into the substrates and the other is reduced to water (monooxygenase reaction).

$$R\text{-}H + O_2 + NAD(P)H + 2\,H^+ \longrightarrow R\text{-}OH + H_2O + NAD(P)^+ \quad (1)$$

The cytochrome $P450_{cam}$ (CYP101) isolated from the soil bacterium *Pseudomonas putida* is a soluble cytosolic enzyme and by using camphor as the only carbon source this organism employs $P450_{cam}$ in order to catalyse the stereospecific hydroxylation at the 5-*exo* position (Scheme 1) as a first step in a cascade of energy supplying reactions. Its feasible isolation, solubility and the possibility to overexpress this enzyme in other bacteria has made $P450_{cam}$ one of the best studied P450

 DOI: 10.1002/adsc.200303011

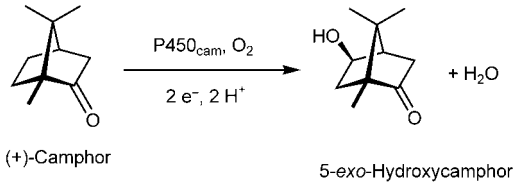

Scheme 1. Hydroxylation of (+)-camphor by $P450_{cam}$ from *Pseudomonas putida*.

systems and for a number of years the high-resolution crystal structure of $P450_{cam}$ (Figure 2) solved by Poulos and co-workers[5a] in 1986 was the only available three-dimensional structure of a P450 enzyme.

The information gained from the X-ray structures of the substrate-free resting state (Figure 2),[5a] the E · S complex with camphor[5b] and substrate analogues,[5c] the structure of the CO adduct,[5d] and the E · P complex with 5-*exo*-hydroxycamphor[5e] of $P450_{cam}$ had a great impact on P450 research. The comparison of these "derivatives" with respect to changes of the spatial arrangements at the active site not only confirmed former indirect spectroscopic evidence but provided important details of substrate binding and clues concerning the mechanism of P450 action. Very recently, in a landmark publication, Schlichting, Sligar and their co-workers have made "snap-shots" of the catalytic cycle of $P450_{cam}$[6] by using rapid data-collection techniques, cryogenic temperatures and long-wavelength X-rays. This work revealed crystal structures of some intermediates of the catalytic cycle which filled important white spots on the map of the $P450_{cam}$ mode of action.

A closer look at the active site of the crystal structure of the resting state of $P450_{cam}$[5a] (Figure 2) revealed that the substrate binding pocket is occupied by a cluster of six hydrogen-bonded water molecules, one of which is coordinating to iron as sixth ligand.

Upon binding of the substrate the water cluster, including the sixth distal water ligand, is completely removed and the camphor molecule is bound by a

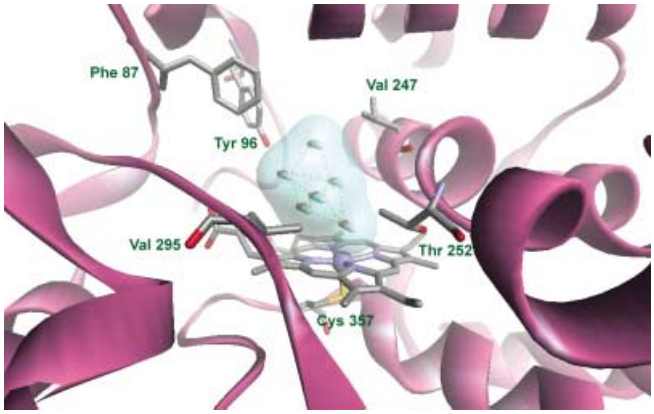

Figure 2. Structure of the active site of the $P450_{cam}$ resting state (PDB entry 1PHC).

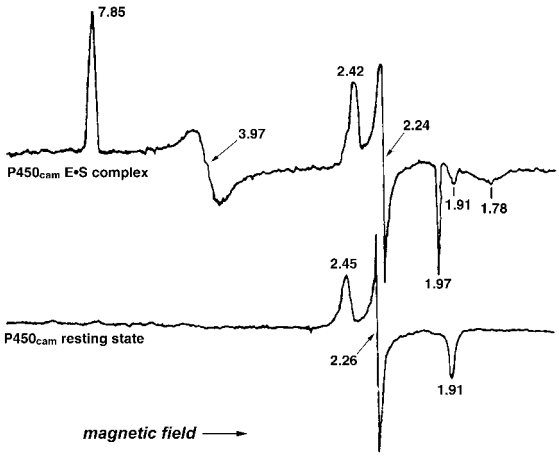

Figure 3. cw-EPR spectra of the resting state (bottom trace) and camphor-bound $P450_{cam}$ (top trace). Spectra were measured in 50 mM potassium phosphate buffer, pH 7.1, 3.5 mM camphor. EPR conditions: $\nu = 9.2$ GHz, $P = 0.5$ mW, $T = 12$ K, modulation frequency 100 kHz, modulation amplitude 12.5 G.

hydrogen bond formed between Tyr96 and the carbonyl group of camphor.

Before the three-dimensional structure of $P450_{cam}$ was elucidated the substrate binding process was studied extensively by spectroscopic methods such as UV-visible spectroscopy,[7] cw-EPR,[8] Mössbauer spectroscopy[9] and electrochemical methods[10] which revealed significant changes upon camphor binding to the resting state of $P450_{cam}$. Substrate binding, for instance, causes a 26 nm blue shift of the *Soret* band in the UV/Vis spectrum of the $P450_{cam}$ resting state.

At 12 K the native cytochrome $P450_{cam}$ is predominantly low-spin ($S = 1/2$) with EPR g values at 2.45, 2.26, and 1.91, but addition of substrate is accompanied by 60% conversion to a rhombically distorted high-spin ($S = 5/2$) form with $g = 7.85$, 3.97, and 1.78 (Figure 3).[8] Mössbauer studies by Sharrock and co-workers confirmed that the binding of camphor to $P450_{cam}$ causes a partial conversion from low- to high-spin.[9] Their data also showed that this spin equilibrium is temperature dependent and the high-spin fraction of camphor-bound $P450_{cam}$ measured at 215 K is approximately 1.6 times that at 4 K which would result in >96% high-spin at room temperature.

The fact that the resting state **1** (Scheme 2) of $P450_{cam}$ is low-spin was very surprising once its crystal structure was solved (Figure 2). It seems unlikely that the thiolate and one of the water molecules, both known to be weak ligands, could establish a low-spin iron complex.

Also, the binding of the camphor alters dramatically the redox potential of the heme iron of $P450_{cam}$ from -300 mV for the resting state to -170 mV with substrate-bound[10] (see **2**, Scheme 2) rendering the latter to accept an electron from NADH *via* the redox

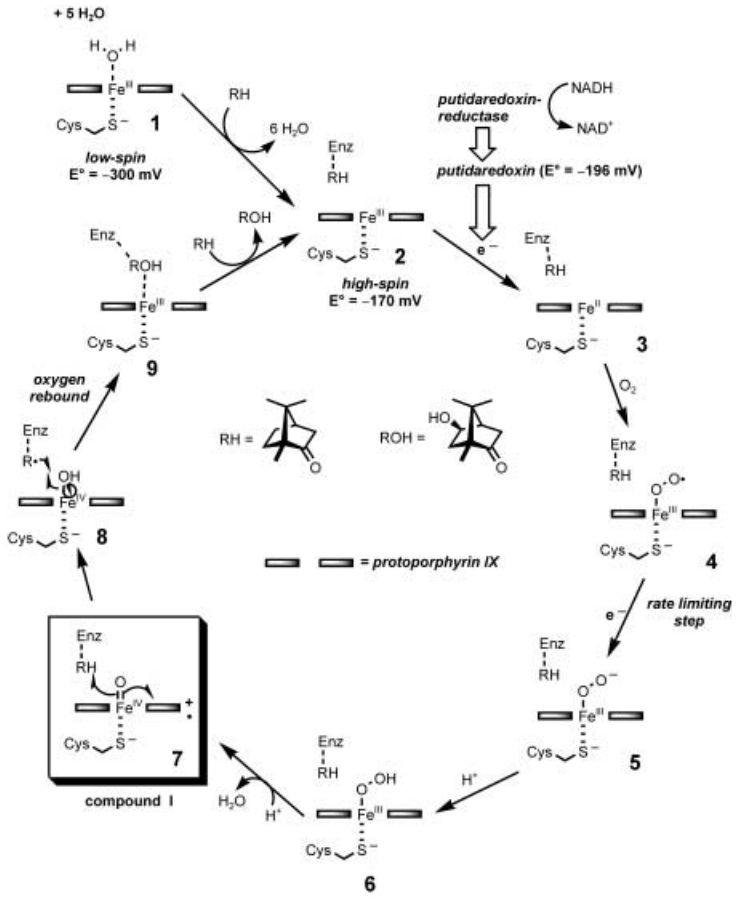

Scheme 2. The consensus mechanism of P450 hydrocarbon hydroxylations.

proteins putidaredoxin reductase (flavoprotein) and putidaredoxin ([Fe-S] protein) which gives rise to a high-spin pentacoordinated Fe^{II} complex **3** (Scheme 2).

The ferrous species **3** is now able to bind molecular dioxygen which results in the diamagnetic low-spin oxy intermediate **4**. A second electron transfer from putidaredoxin to **4** forms the ferric peroxo complex **5**. In the rebound mechanism proposed by Groves et al.[11] the distal oxygen atom of the peroxo complex **5** is protonated twice, first to give a hydroperoxide complex **6** and then to induce a heterolytic O–O bond cleavage, releasing water and generating the oxo-ferryl (Fe^{IV}) porphyrin radical cation intermediate **7** which is equivalent to the high-valent iron-oxo species of peroxidase enzymes, historically described as compound I.[12] The highly reactive species **7** abstracts a hydrogen atom from the enzyme bound substrate yielding a carbon-centred radical with a finite lifetime and hydroxo ferryl complex **8**. In the following *oxygen rebound* step the oxygen atom is transferred to the enzyme-bound substrate radical which results in the formation of the low-spin ferric enzyme-product complex **9**. Finally, dissociation of the product closes the catalytic cycle.

It is evident that the spin equilibrium triggers the entry into the catalytic cycle. Furthermore, the low-spin state of the resting state **1** is crucial for the function and efficiency of the P450 enzyme since this control mechanism prevents unnecessary flow of electrons into the catalytic cycle if no substrate is bound and hence suppresses uncoupling (formation of H_2O_2). Numerous theoretical studies of the Shaik group suggest that compound I (**7**) is a chameleon species, that may tune its reactivity and selectivity patterns in response to the substrate and the protein environment in which it is accommodated.[13] According to their calculations, compound I of P450 is a two-state reagent having closely lying quartet ($^4A_{2u}$, high-spin) and doublet states ($^2A_{2u}$, low-spin). Moreover, C-H hydroxylation is following the two-state reactivity (TSR) scenario[14] and reactivity patterns and product distribution are determined by the interplay of the two states which itself depends on the spin-crossover from high-spin to low-spin, on the environment (the shape of the substrate binding pocket of the enzyme used, its acidity, polarity, etc.[13a, d]) and finally on the substrate. Hence, spin state changes also trigger the mode/reactivity of oxygen insertion by the compound I species.

Contradictory arguments have been published to explain the origin of the low-spin resting state of $P450_{cam}$. On one hand, Poulos et al.[15] suggested that

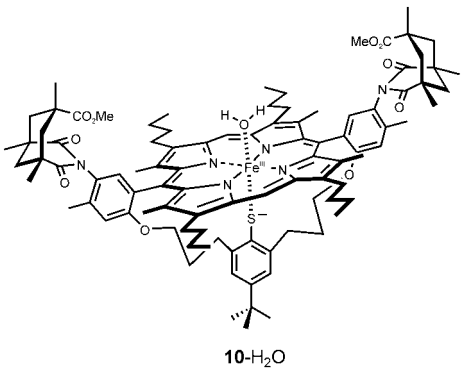

10-H_2O

Figure 4. Previous high-spin active site analogue **10**-H_2O for the resting state of $P450_{cam}$.

polarisation of the coordinated water molecule through the hydrogen bonding network in the water cluster could result in a distinctive hydroxide character (strong ligand) and thus lead to a low-spin complex. On the other hand by comparing simulated and experimental ^{17}O ESEEM and pulsed ENDOR/four-pulse ESEEM spectra of the resting state of $P450_{cam}$, Goldfarb et al.[16] concluded that the distal ligand is a water molecule rather than a hydroxide ligand. Semiempirical calculations by Loew and Harris[17a] suggested a significant contribution of the electrostatic field of the surrounding protein stabilising the low-spin resting state. It was proposed by the same authors that a point charge above the porphyrin plane would simulate the electrostatic field of the protein and push the spin equilibrium towards low-spin.[17b]

Using various EPR techniques it was previously shown in our group that the active site analogue **10**-H_2O (Figure 4)[18a] is definitely high-spin and only changes to the low-spin state if the coordinating water is replaced by 1,2-Me_2Im.[18b] These results clearly indicated that the coordination of water to Fe(III) of the heme thiolate cofactor is insufficient to stabilise the low-spin state of the resting state of $P450_{cam}$.

In order to unravel the origin of the low-spin resting state of $P450_{cam}$ our aim was to synthesise and characterise active site analogues of this enzyme that mimic (i) the proposed polarisation effect[15] in the water cluster and (ii) the influence of the electrostatic field from the surrounding protein as suggested by calculations.[17a] From the design point of view we thought that the former could be achieved by placing hydrogen bond acceptors near the distal site of the porphyrin which can form hydrogen bonds with the water molecule coordinating to the iron. The latter effect was thought to be mimicked by attaching a point charge above the porphyrin plane which would push the spin equilibrium towards low-spin.

Results and Discussion

Synthesis and Study of the Bis(tetrahydrofuranyl) Iron(III) Porphyrin – a First Model for Mimicking the Polarisation Effect in the Water Cluster

The bis-THF model **11** was considered being suitable to polarise a coordinated water molecule *via* hydrogen bonding whereby the ether oxygens act as H-bond acceptors (Scheme 3). Therefore, **11** should be an active site analogue to mimic the polarisation effect in the water cluster of the native enzyme. Retrosynthetic analysis leads to bis(aminophenyl)porphyrin **12** and tetrahydrofurancarbonyl chloride **13**[19] which, in turn, would be synthesised from the corresponding acid **14**. The bis(aminophenyl)porphyrin can be disconnected to the following three fragments: dipyrromethane **15**[18a], protected aldehyde **16** and activated and protected thiophenyl bridge **17**.[18]

The synthesis started from commercially available *m*-anisidine (**18**) the amino function of which was first protected as the *tert*-butoxycarbamate (Scheme 4). Formylation of **19**[20] was achieved following a protocol by Stanetty et al.[21] whereby the methoxy and the carbamate group direct the formylation to the 2-position. Saponification of **20**[22] and subsequent decarboxylation of the resulting diacid **21** yielded the air- and light-sensitive dipyrromethane **15** which was immediately used in the next step. Classical porphyrin condensation[23] of dipyrromethane **15** and aldehyde **16** under acid catalysis with *p*-toluenesulphonic acid gave after subsequent oxidation of the formed porphyrinogens with

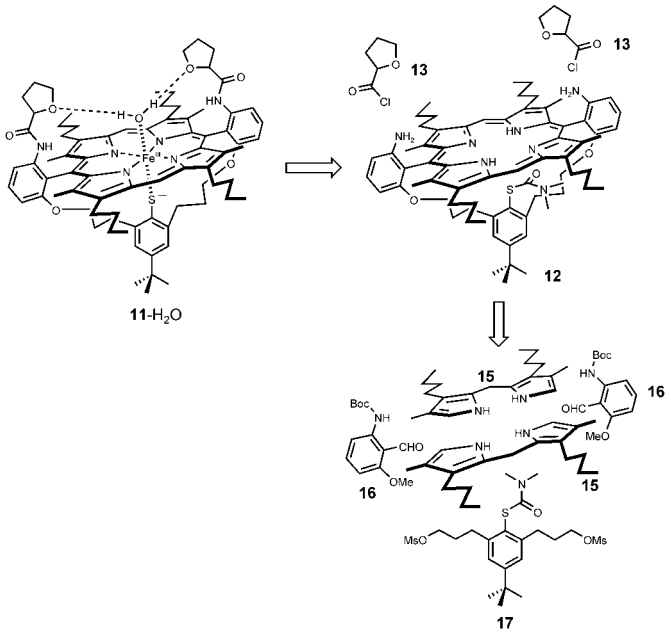

Scheme 3. Retrosynthetic analysis of tetrahydrofuranyl iron porphyrin model **11**.

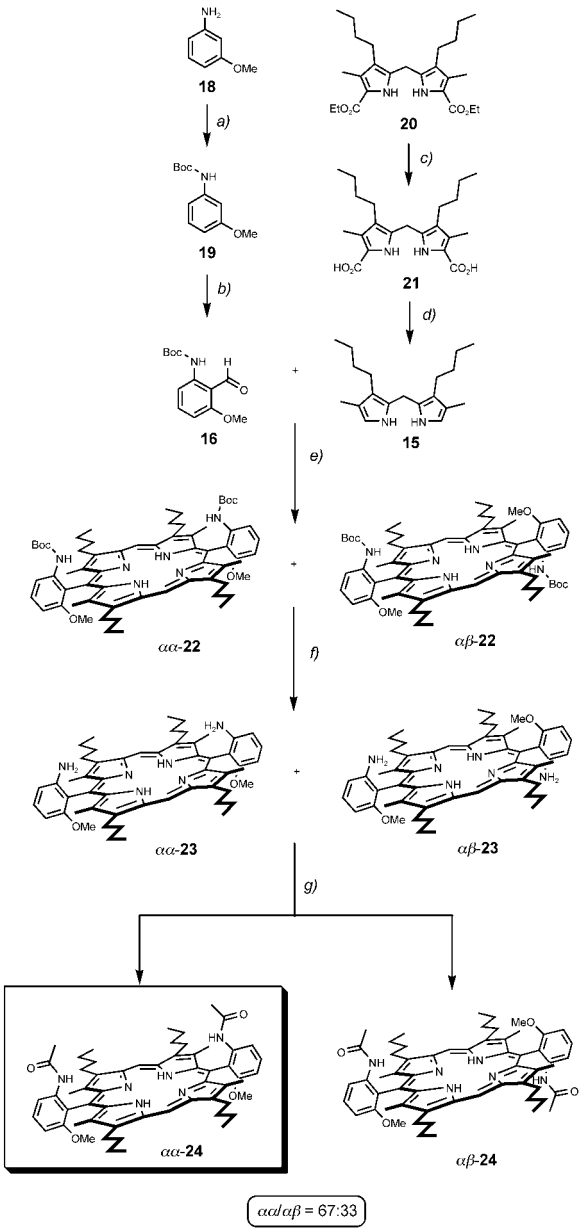

Scheme 4. Synthesis of tetrahydrofuranyl model **11** – porphyrin condensation. *Reagents and conditions:* (a) Boc_2O (1.6 equivs.), THF, rt, overnight, quant. (b) *t*-BuLi (2.2 equivs.), Et_2O, $-10\,^{\circ}C$, 3 h; then DMF (2 equivs.), Et_2O, $-78\,^{\circ}C \rightarrow$ rt, overnight, 82%. (c) NaOH (5 equivs.), EtOH/H_2O, reflux, 4 h, 92%. (d) $H_2N(CH_2)_2OH$, $120\,^{\circ}C$, 45 min, 57%. (e) *cat*. *p*-TsOH, MeCN, rt, overnight; then DDQ (2 equivs.) in THF, rt, 1.5 h. (f) TFA (82 equivs.), CH_2Cl_2, rt, 12.5 h, 40% (2 steps). (g) AcCl (2.5 equivs.), pyridine (3.3 equivs.), *cat*. DMAP, CH_2Cl_2, rt, 18 h; then flash chromatography, 49% αα-**24**, 24% αβ-**24**.

DDQ a mixture of two atropisomers, αα-**22** and αβ-**22**, respectively. This mixture was treated with trifluoroacetic acid to remove the protecting groups and the liberated amino functions of αα-**23** and αβ-**23** were reprotected with the acid-stable acetylamino group. At this stage it was possible to separate the two atropisomers by flash chromatography on silica gel which yielded pure αα-**24** in 49% as the more polar fraction and αβ-**24** in 24% as the less polar compound. This results in a ratio of αα/αβ ~ 67:33 which was virtually the same ratio as deduced from RP-HPLC of the atropisomeric mixture αα/αβ-**24**.

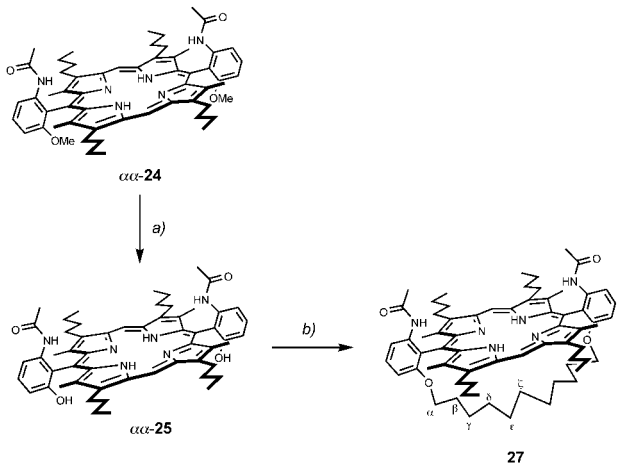

Scheme 5. Chemical derivatisation of bisphenol porphyrin αα-**25** for atropisomer assignment. *Reagents and conditions:* (a) $AlCl_3$ (38 equivs.), $EtSH/CH_2Cl_2$ (3:2), rt, 43 h, 73%. (b) Cs_2CO_3 (30 equivs.), DMF, $60\,^{\circ}C$, 30 min; then $Br(CH_2)_{11}Br$ (1.5 equivs.), DMF, $60\,^{\circ}C$, high-dilution, 3 h, 63%.

If one is looking at the overall yield of αα-**24** (20% from aldehyde **16**) it seems very low at first glance but it is in the typical range of porphyrin condensations (10–30%) compared to examples in the literature. The synthesis was now continued with the αα-atropisomer of **24** and cleavage of the methyl ethers was carried out with anhydrous aluminium chloride in a solvent mixture of CH_2Cl_2 and EtSH. This gave bisphenol porphyrin αα-**25** in good yield (Scheme 5).

It is worth noting that, in contrast to isomers such as αα-**26**[18a], the atropisomers of this series of porphyrins, due to steric congestion between the substituents at the β-pyrrole positions and the substituents at the 2′- and 6′-positions of the phenyl rings, are configurationally stable during manipulations or purification (Figure 5). To distinguish between atropisomers such as αα-**24** and αβ-**24** ^1H NMR analysis is insufficient due to very small differences in chemical shift pattern. Also polarity arguments taken from TLC behaviour of similar compounds[24] proved to be ambiguous.

Therefore it was decided to pursue a macrocyclisation which could be easily done with αα-**25** but would be impossible to perform with αβ-**25**. In the event, the porphyrin, tentatively assigned as αα-**25** was bridged with 1,11-dibromoundecane in the presence of Cs_2CO_3 in hot DMF under high-dilution conditions (Scheme 5). It is known that eleven carbon atoms are sufficient to span the porphyrin plane[25] and furthermore the αβ-

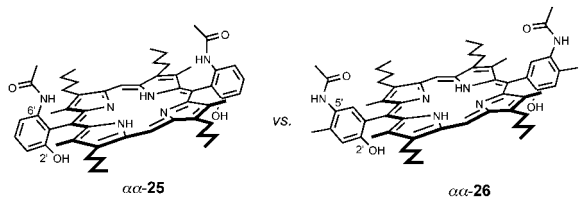

Figure 5. Comparison of configurational stability of porphyrins with different substitution at the *meso*-phenyl rings.

isomer of **25** cannot form a macrocyclic structure. As observed in ^{1}H NMR successful bridging of αα-**25** was confirmed by the high-field shifted signals for the methylene groups of the undecanylene strap of **27** due to the ring current of the porphyrin (α-CH_2 3.82 ppm, β-CH_2 0.70 ppm, γ-CH_2 −0.34 ppm, δ-CH_2 −0.67 ppm, ε-CH_2 and ζ-CH_2 −1.61 ppm, respectively).

Accordingly, the correct atropisomer was identified and the synthesis continued with the bridging of αα-**25** with activated and protected thiophenylene **17** under high-dilution conditions in hot DMF in the presence of Cs_2CO_3 (Scheme 6). The latter reagent acts on one hand as a base to preform the bisphenolate and on the other hand has a templating effect for macrocyclisation.[25] The dimesylate **17** was synthesised from the corresponding diol **29** which was obtained *via* hydroboration reaction of diallylthiophenol carbamate **28**.[25] The distal acetylamino groups were hydrolysed by refluxing **30** in a mixture of 6 M HCl and MeOH to give bis(aminophenyl) porphyrin **12** in high yield.

The bis(aminophenyl) porphyrin **12** (9% overall yield for longest linear sequence starting from *m*-anisidine **18**) is a very useful building block because the free amino groups can be functionalised in many different ways and lead to thiophenolate-bridged iron(III) porphyrins with various functionalities in the distal site. By this strategy it is possible to have access to model compounds mimicking different active sites of enzymes having a heme cysteinate cofactor like cytochrome P450 s, chloroperoxidase (CPO) and nitric oxide synthase (NOS).[18,25,26]

In the case of the bis(tetrahydrofuranyl) model **11** the amino groups were acylated with tetrahydrofurancarbonyl chloride **13** which was obtained from the corresponding acid **14** by treatment with oxalyl chloride (Scheme 7). Cleavage of the thiocarbamate protecting group of **31** liberated the thiophenol function and subsequent iron insertion using $FeBr_2$ in the presence of 2,6-lutidine as base in refluxing toluene completed the synthesis of bis(tetrahydrofuranyl) model **11**.

Upon iron insertion the *Soret* band in the UV/Vis blue-shifts from 412 nm for **32** to 406 nm for iron(III) compound **11**. Furthermore, the correct mass of the

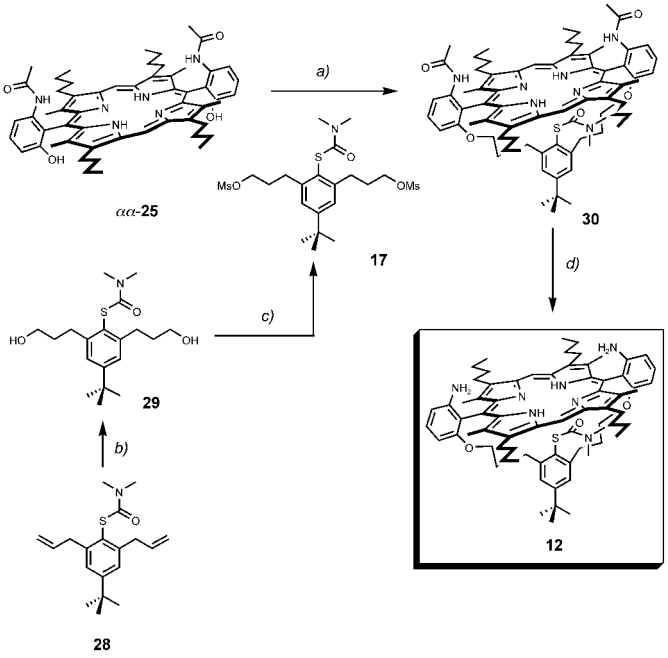

Scheme 6. Synthetic route to bridged bis(aminophenyl) porphyrin **12**. *Reagents and conditions:* (a) Cs_2CO_3 (30 equivs.), DMF, 60 °C, 30 min; then **17** (1.5 equivs.), DMF, 60 °C, 4.5 h, high-dilution, 85%. (b) $BH_3 \cdot Me_2S$ (3.6 equivs.), THF, rt, 3 h; then 3 M NaOH, 10% aqueous H_2O_2, reflux, 1 h, 77%. (c) MsCl (4.7 equivs.), Et_3N (8 equivs.), CH_2Cl_2, 0 °C → rt, 3 h, 96%. (d) 6 M HCl/MeOH, reflux, 2 h, 91%.

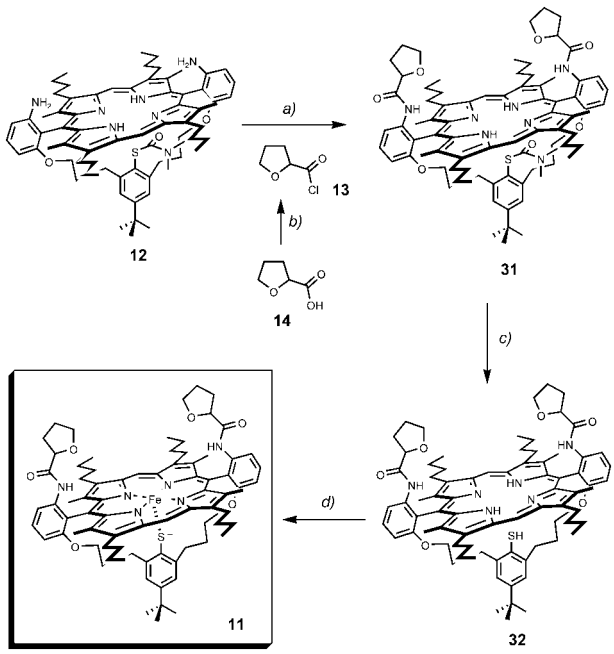

Scheme 7. Completion of the synthesis of tetrahydrofuranyl model **11**. *Reagents and conditions:* (a) **13** (4 equivs.), Et_3N (4.8 equivs.), *cat*. DMAP, CH_2Cl_2, rt, 13 h, 92%. (b) oxalyl chloride, rt, 22 h, 94%. (c) KOMe in MeOH (2.2 M, 59 equivs.), dioxane, reflux, 15 min, 73%. (d) $FeBr_2$ (9 equivs.), 2,6-lutidine (17 equivs.), toluene, reflux, 1 h, 92%.

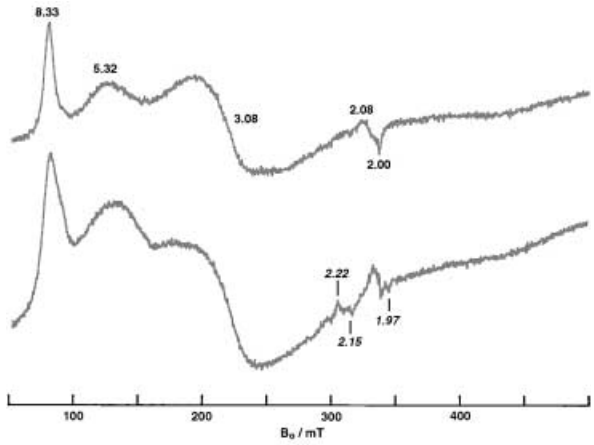

Figure 6. cw-EPR spectra of tetrahydrofuranyl model **11** in dry toluene (top trace) and in water-saturated toluene (bottom trace). Conditions: $\nu = 9.46$ GHz, $P = 20$ mW, $T =$ 100 K, modulation frequency 100 kHz, modulation amplitude 5.2 G.

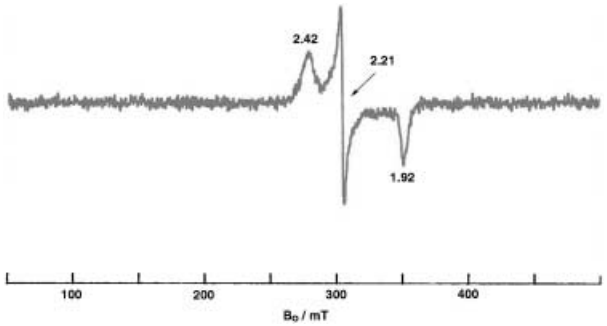

Figure 7. cw-EPR spectra of imidazole complex **11**-Im in DMF. Conditions: $\nu = 9.39$ GHz, $P = 20$ mW, $T = 104$ K, modulation frequency 100 kHz, modulation amplitude 5.2 G.

isolated iron(III) porphyrin model compound **11** was confirmed by ESI-MS and MALDI-TOF-MS.

The cw-EPR spectrum of **11** in dry toluene at low temperature showed g values (8.33, 5.32, 3.08, 2.08 and 2.00) characteristic of pure high-spin iron(III) porphyrins with a strong rhombic distortion (Figure 6, top trace). If this compound was stirred in water-saturated toluene at room temperature for 2.5 days (Scheme 8) cw-EPR analysis of the resulting solution revealed very weak rhombic low-spin signals with g values of 2.22, 2.15 and 1.97 (Figure 6, bottom trace). Even though the amount of low-spin signals was very small this result clearly showed that ether oxygens, when placed in a proper distance in the distal site, can act as hydrogen bond acceptors, polarising the water molecule which coordinates to the central metal and hence leading to a hydroxide character.

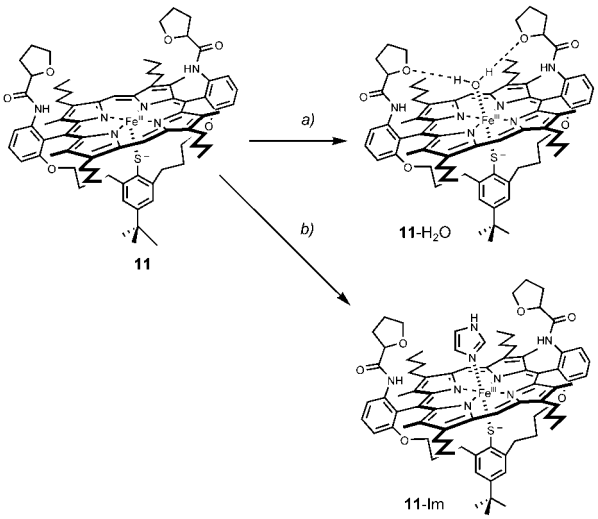

Scheme 8. Complexes of active site model **11**. *Reagents and conditions:* (a) water-saturated toluene, rt, 62 h. (b) ImH (100 equivs.), DMF, rt, 20 h.

A purely rhombic low-spin cw-EPR spectrum, although with slightly different g values (2.42, 2.21, 1.92), can be obtained if iron(III) porphyrin **11** is treated with an excess of imidazole which is known to be a strong ligand with a high affinity towards iron(III) porphyrins (Scheme 8 and Figure 7). This result confirms a general trend obvious from an earlier experiment using **10**-H_2O, see Figure 4, which on treatment with 1,2 dimethylimidazole also changes completely to a low-spin system.[18b]

It is essential to carry out the deprotection reaction of **31** and the iron insertion under strict exclusion of dioxygen because it is well known from previous work in our group that the sulphur of the thiophenolate is prone to oxidation to give the $Fe^{III}(porph)(ArSO_3^-)$ compound[27]. In practice, the deprotection reactions, the work-up and the purification of **31** were done under argon with degassed solvents and reagents. The iron insertions and all further reactions with the iron(III) porphyrins were performed in a glove box with inert atmosphere and degassed solvents and reagents.

Of course, **31** consists of a mixture of four stereoisomers. Separation of diastereoisomers was not done at this stage since the subsequent deprotection reaction under strongly basic conditions (59 equivalents of KOMe in refluxing dioxane) leads to epimerisation at the stereogenic centres. The resulting *RR*,*SS*-**32** and *RS*,*SR*-**32** were separated by flash chromatography displaying distinct ^{1}H NMR spectra due to their different symmetries. Pure *RR*,*SS*-**32** was used for iron insertion to yield *RR*,*SS*-**11**; note that 2,6-lutidine is too weak a base to cause epimerisation at chirality centres of the tetrahydrofuran subunits. The spectroscopic characteristics and the cw-EPR behaviour in the presence of water were the same as for the diastereoisomeric mixture of **11**, see above.

Crown-Capped Iron Porphyrins – Models for the Electrostatic Field Effect and the Polarisation Effect in the Water Cluster

On one hand the results with the tetrahydrofuranyl model **11** pointed out that ether oxygens near the distal site of an iron(III) porphyrin can act as hydrogen bond acceptors for a coordinated water molecule. On the other hand we were looking for a model which mimics the electrostatic field effect. Crown-capped iron(III) porphyrins **33** (n = 1) and **34** (n = 2) combine these two required criteria in one molecule (Scheme 9).

The 1,10-diaza-18-crown-6 is known to bind divalent cations such as Ba^{2+}[28] which would place a point charge above the porphyrin plane and allow the investigation of the electrostatic field effect on the iron(III) spin state. It was considered to choose a divalent cation in order to have a larger amount of charge since upon binding of cations to crown ethers the charge is normally slightly shielded. In addition, the element providing the cation should not have isotopes with nuclear spin I = 1/2 or 3/2 which would complicate cw-EPR analysis or provoke spin-spin interactions with the paramagnetic iron(III). Moreover, the oxygens of the crown ether can act as hydrogen bond acceptors[29] to water coordinated to the iron(III) if placed in a proper distance. Because this critical distance is difficult to estimate by molecular modelling, a crown-capped model **33** (n = 1) with a C_1-linker and active site model **34** (n = 2) with a C_2-linker were designed and synthesised. Retrosynthetic disconnections are shown in Scheme 9 and simplified crown-capped models **33** and **34** to 1,10-diaza-18-crown-6 (**35**), 2-chloroacetyl chloride for **33**, acryloyl chloride for **34** and the already synthesised bis(aminophenyl) porphyrin **12**.

For the capping of the distal face of the porphyrin we took advantage of published procedures of Collman et al.[30] and Guilard et al.[29] In the event, bis(aminophenyl)porphyrin **12** was acylated with either 2-chloroacetyl chloride or acryloyl chloride which provided the bisamide porphyrins **36** (R = CH_2Cl) and **37** (R = $CH{=}CH_2$) as depicted in Scheme 10. Both compounds, especially bis(acrylamido)porphyrin **37** are quite sensitive and should be used as soon as possible in the next step. The capping with diazacrown ether **35** proceeded *via* a congruent double substitution reaction to give **38** or *via* a congruent double Michael addition which furnished **39**. In both cases the capped products **38** and **39** were obtained in surprisingly good yields (68% and 66%, respectively).

Regarding the yield for reactions on a larger scale it proved to be advantageous in the case of **38** to use the crude bis(amidophenyl)porphyrin **36** in the subsequent reaction and to purify after the capping step (see Experimental Section for details).

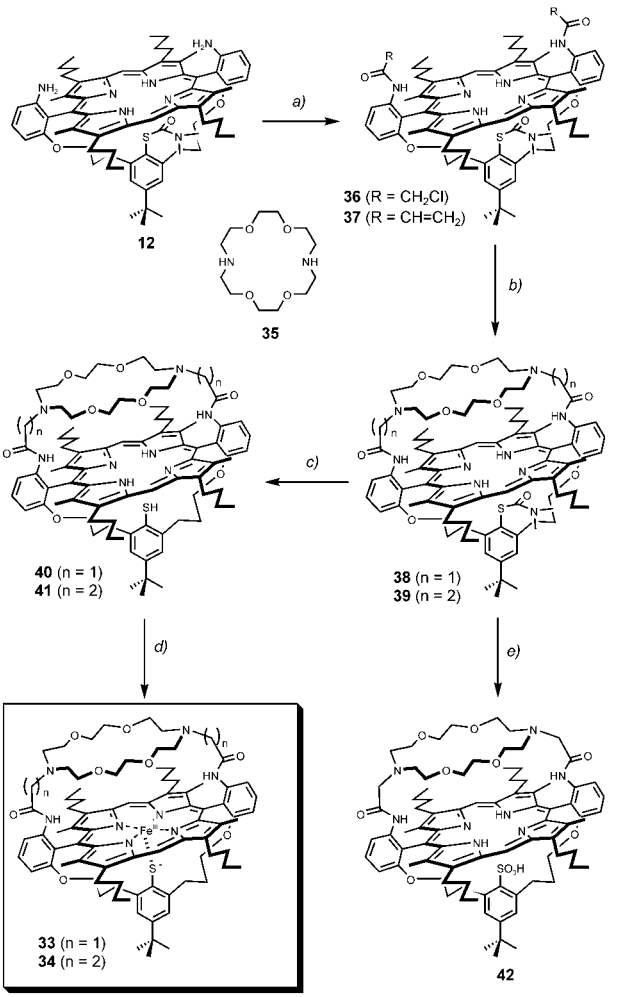

Scheme 10. Synthesis of crown-capped active site analogues **33** and **34**. *Reagents and conditions:* (a) for n = 1 : 2-chloroacetyl chloride (3.8 equivs.), Et_3N (4.8 equivs.), *cat*. DMAP, CH_2Cl_2, rt, 15 min, 61% **36**; for n = 2: acryloyl chloride (2.4 equivs.), Et_3N (27 equivs.), CH_2Cl_2, rt, 4.5 h, 72% **37**. (b) for R = CH_2Cl: **35** (5 equivs.), EtOH, reflux, 21 h, 68% **38**; for R = $CH{=}CH_2$: **35** (5 equivs.), MeOH/CH_2Cl_2 25 : 1, reflux, 44 h, 66% **39**. (c) KOMe in MeOH (10 equivs.), dioxane, reflux, 10 min, 48% **40**, 81% **41**. (d) $FeBr_2$ (11 equivs.), 2,6-lutidine (20 equivs.), toluene, reflux, 30 min, 92% **33**, 58% **34**. (e) solid KOMe (60 equivs.), dioxane, reflux, 10 min, 54%.

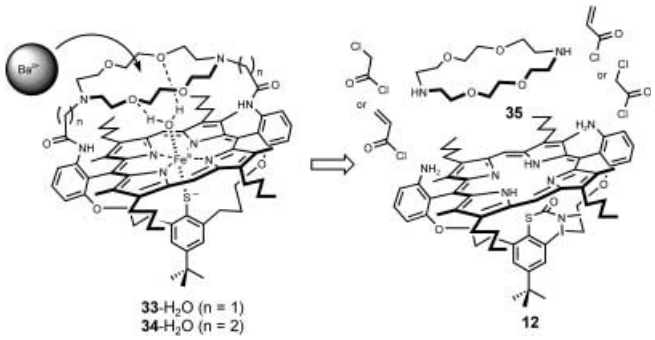

Scheme 9. Retrosynthetic analysis of crown-capped porphyrins **33** and **34**.

Table 1. Proton chemical shifts[a] of crown ether methylene groups of **40** and **41**.

Compound	δ_H a-NCH_2	δ_H b-OCH_2	δ_H c-OCH_2
40	0.45, −0.17	1.44, 1.59	1.76
41	0.10	1.04	1.98

[a] All chemical shifts in ppm relative to residual solvent peak. Spectra were recorded at 298 K in $CDCl_3$.

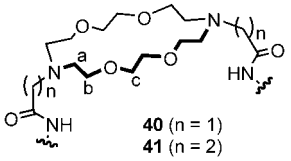

Figure 8. Atom numbering of the diazacrown cap.

As in the case of tetrahydrofuranylporphyrin **31** the thiocarbamate protecting groups of **38** and **39** were cleaved off by treatment with KOMe in refluxing dioxane. Again, it is absolutely essential that this reaction is carried out under strict exclusion of dioxygen and using a freshly prepared KOMe solution (in MeOH) instead of solid KOMe. For instance, a substantial amount of or even only the *S*-oxidised product **42** was isolated if the cleavage reaction of **38** was not done carefully enough. Furthermore, the oxidised product **42** was very difficult to separate from **40**.

Due to the bulky thiocarbamate protecting group the conformational freedom of the sulphur bridge tethered to the porphyrin macrocycle is largely reduced. This results in a reduced symmetry and thus to very complicated ^{1}H NMR spectra, especially in the cases of **31**, **38** and **39**. Once the sulphur protecting group is cleaved off the symmetry increases and allows interpretation of the ^{1}H NMR spectra. In addition, homo- and heterocorrelated 2D NMR techniques were very helpful to assure the full assignment of all signals and together with supportive data from MALDI-TOF-MS and ESI-MS to confirm the structures. Due to the ring current of the porphyrin the methylene groups of the crown ether are high-field shifted (Table 1 and Figure 8) which is another indication of a successfully capped structure.

The ^{1}H NMR of the *S*-oxidised crown-capped porphyrin **42** also shows a spectrum with high symmetry which leads to the conclusion that the oxidation happens only at sulphur. In contrast, oxidation of the porphyrin ring (e.g., at the *meso*-positions) should result in a spectrum with reduced symmetry and different UV/Vis and mass spectra.

After having assured the structures of **40** and **41** iron insertion was carried out under standard conditions affording crown-capped iron(III) porphyrins **33** and **34** (Scheme 10). The yield was much lower if using crown-capped porphyrin **41** with the C_2-linker and dropped drastically if the reaction was carried out on a larger scale (>10 mg). Judging from TLC decomposition is taking place during the iron insertion reaction with **41**. One reason could be a retro-Michael reaction which is initiated by the base present (20 equivalents of 2,6-lutidine) giving the bis(acrylamidophenyl)porphyrin **37** which as such is unstable as already experienced during the synthesis of the crown-capped models (*vide supra*). The observation that iron insertion of crown-capped porphyrin **40** with the C_1-linker gives very good yields and is not accompanied by decomposition supports this suggestion since such a side reaction is not possible in the case of **40**. Both iron(III) porphyrins **33** and **34** showed characteristic physical data (Table 2).

cw-EPR Study of Crown-Capped Iron(III) Porphyrins and of Their Water Complexes – Mimicking the Polarisation Effect of the Water Cluster

In dry toluene both **33** and **34** showed cw-EPR spectra characteristic of pure high-spin iron(III) porphyrins with a strong rhombic contribution from the ligand field (Figure 9a and 9b, top traces).

The cw-EPR spectrum of **34** in water-saturated toluene was identical with the spectrum in dry toluene (Figure 9b, bottom trace). In contrast, when **33** was measured in water-saturated toluene low-spin signals in the cw-EPR spectrum appeared (Figure 9a, bottom trace). These g values are very similar to those obtained for the low-spin resting state of cytochrome $P450_{cam}$ ($g = 2.45, 2.26, 1.91$, Figure 3)[8] and to those obtained for the imidazole complex **11**-Im ($g = 2.42, 2.21, 1.92$, Figure 7). A sample of **33** in water-saturated toluene was periodically measured over a time period of 24 h to see if there is an increase in intensity of the low-spin signals but this was not the case. It was calculated that in a typical 5 mM

Table 2. Physical data of iron(III) porphyrins **33** and **34**.

Compound	UV/Vis[a] [nm]	MALDI-TOF-MS [*m/z*]	ESI-MS[b] [*m/z*]
33	404	1447 $[M+2]^+$	1469 $[M+Na]^+$
34	406	1475 $[M+1]^+$	1497 $[M+Na]^+$

[a] In toluene at 298 K.
[b] In MeOH.

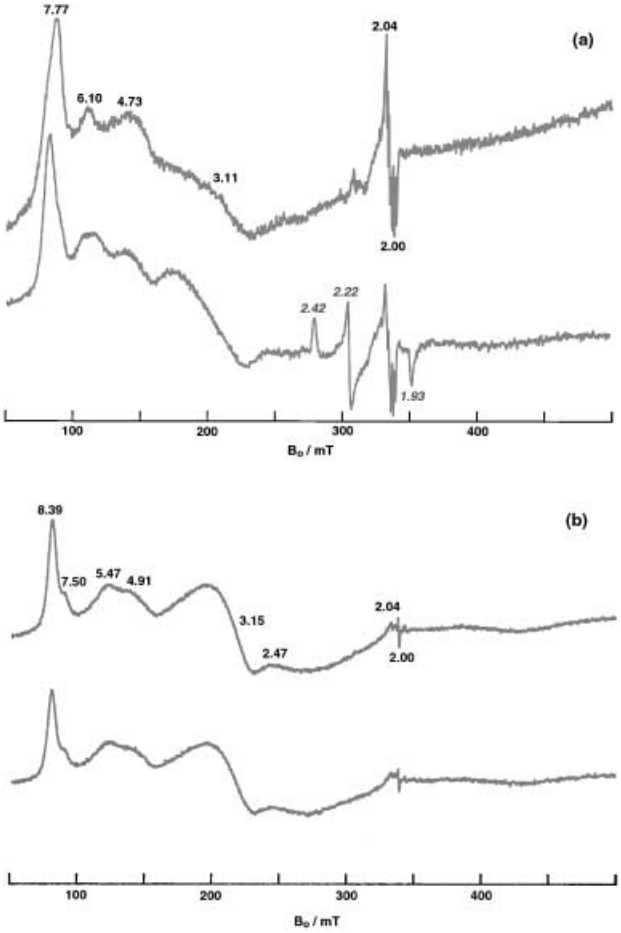

Figure 9. cw-EPR spectra of crown-capped models **33** (**a**) and **34** (**b**) in dry toluene (top traces) and in water-saturated toluene (bottom traces). Conditions: $\nu = 9.46$ GHz, $P = 20$ mW, $T = 100$ K, modulation frequency 100 kHz, modulation amplitude 5.2 G.

cw-EPR iron(III) porphyrin sample in water-saturated toluene only ~ 3–4 equivalents of water are present, thus it is not surprising that the system does not convert completely to low spin. In water-saturated 2-MTHF cw-EPR spectra of **33** (not shown) displayed the same low-spin signals albeit with lower intensity.

Guilard and co-workers have prepared a crown-capped zinc porphyrin[29] which has the same distal architecture as crown-capped model **33** and they were able to solve the crystal structure of the corresponding water complex. This analysis revealed that the water molecule was bound to the central Zn(II) ion and was hydrogen bonded to two crown ether oxygens with hydrogen bond distances of 1.95 Å and 1.83 Å. It is reasonable to assume that water binds in the same fashion to crown-capped iron(III) porphyrin **33** (Figure 10) and these hydrogen bonds presumably polarise the coordinated water molecule leading to a distinctive hydroxide character which gives rise to low-spin signals in the cw-EPR spectrum of **33** in water-saturated

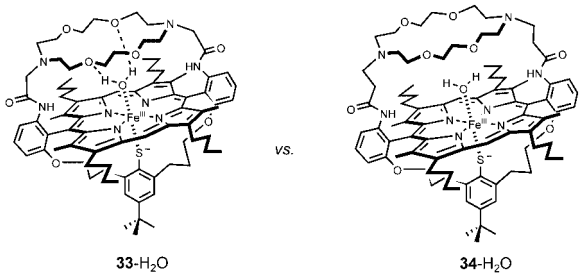

Figure 10. Different water binding motives of crown-capped models **33** and **34**.

toluene. In contrast, due to the different length of the linker of crown-capped iron(III) porphyrin **34** hydrogen bonding is not possible and therefore only high-spin signals are observed in the cw-EPR spectrum.

As for to the bis(tetrahydrofuranyl)iron(III) porphyrin **11** we tried to generate low-spin imidazole complexes of the crown-capped iron(III) porphyrin models. The model compound **34** was chosen due to the longer C_2-linkers and hence better accessibility of the imidazole to the central metal and treated with a large excess of the ligand (Scheme 11). The analysis by cw-EPR showed low-spin signals with g values of 2.45, 2.21 and 1.91 which were very similar to g values found for the imidazole complex **11**-Im, however, displaying much lower intensity (Figure 11).

For yet unknown reasons attempts to prepare the hydroxide complex ($HO^- - Fe(III) - S^-$) from either **33**-H_2O or **34**-H_2O failed. In contrast we have been able to prepare the required adduct from **10**-H_2O, see Figure 4, by deprotonation with ethyldiisopropylamine. As expected the cw-EPR of **10**-OH^- showed a complete conversion to a low-spin system displaying g values = 2.20, 2.02, 1.95. The coordination features of the "open-face" iron thiolate porphyrins **10** and **11** versus the "crown-capped" complexes **33** and **34** suggest that the latter are sterically much more congested such that the sixth coordination site of iron(III) is much less accessible than molecular modelling predicts.

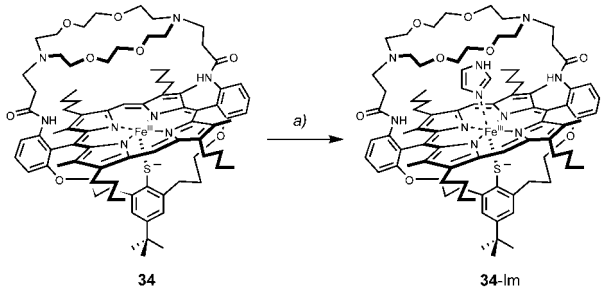

Scheme 11. Synthesis of crown-capped imidazole complex **34**-Im. *Reagents and conditions:* (a) ImH (100 equivs.), DMF, rt, 39 h.

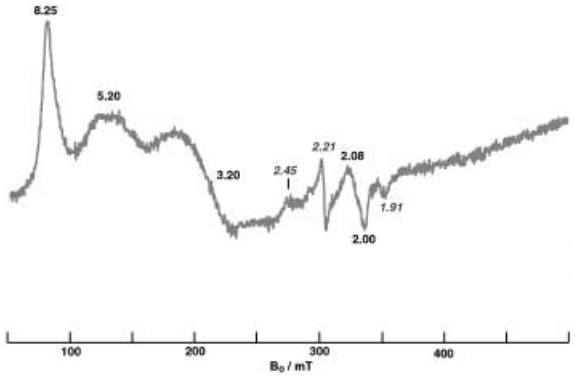

Figure 11. cw-EPR spectra of reaction mixture in DMF after treatment of **34** with excess of imidazole. Conditions: $\nu = 9.39$ GHz, $P = 20$ mW, $T = 104$ K, modulation frequency 100 kHz, modulation amplitude 5.2 G.

cw-EPR and ESI-MS Studies of Barium Complexes of Crown-Capped Iron(III) Porphyrins – Mimicking the Electrostatic Field Effect

If solutions of crown-capped iron(III) porphyrins **33** and **34** in acetone were treated with 5 equivalents of $Ba(ClO_4)_2$ and the resulting solutions were ultrasonicated the ESI-MS analysis of the mixtures revealed mass peaks for the corresponding complexes next to the $[M + H]^+$ and $[M + Na]^+$ peaks (Figure 12, insets). However, binding of barium(II) ions did not change the cw-EPR spectra of the compounds. In fact, model compound **34**-H_2O/Ba^{2+} with C_2-linkers remains high-spin in water-saturated toluene as well as in acetone (Figure 12b) and **33**-H_2O/Ba^{2+} shows the same content of low-spin in water-saturated toluene as **33**-H_2O (Figure 12a).

It is difficult to estimate to what extent the charge of the bound barium(II) ion is shielded by the diazacrown ether and in organic solvents like toluene the counterion perchlorate is probably in close proximity to the barium(II) which may further decrease the point charge. Such ion paired $[M + Ba + ClO_4]^+$ species are even detectable in ESI-MS (Figure 12, insets). Therefore, in order to increase the dipole-distance between the barium(II) and the counterion the perchlorates were exchanged by the large, lipophilic TRISPHAT anions developed by Lacour et al.[31] Barium(II) complex **33**-Ba^{2+} was treated with (Bu_3NH)[TRISPHAT][32] in CH_2Cl_2 and the resulting solution was used for the analysis. Gratifyingly, the desired mass peaks could be detected by ESI-MS (Figure 13) but the cw-EPR spectrum of this solution in water-saturated toluene showed a high content of rhombic high-spin signals and very little to no content of low-spin signals (not shown).

Taken together, the experiments point to the fact that a positively charged barium(II) ion attached above the porphyrin ring does not have a significant influence on the spin state of the iron(III).

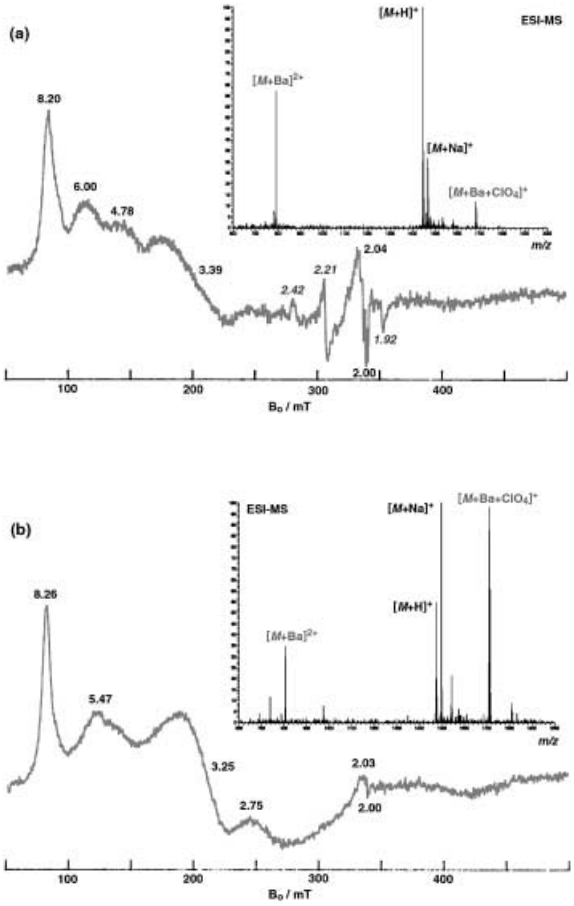

Figure 12. cw-EPR spectra of **33** in water-saturated toluene (**a**) and of **34** in acetone (**b**) after addition of 5 equivalents of $Ba(ClO_4)_2$. Insets: corresponding ESI-MS in acetone. EPR conditions: $\nu = 9.47$ GHz, $P = 20$ mW, $T = 100$ K, modulation frequency 100 kHz, modulation amplitude 5.2 G.

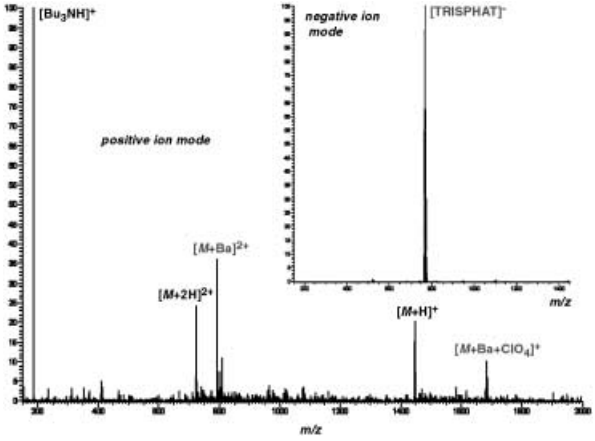

Figure 13. Positive ion mode ESI-MS in acetone after anion exchange of **33**-Ba^{2+} with 2 equivalents of (Bu_3NH) [TRISPHAT]; inset: same sample at negative ion mode.

In order to study an alternative model for the electrostatic field effect our attention was drawn to the idea with a fixed charge above the porphyrin plane. Inspired

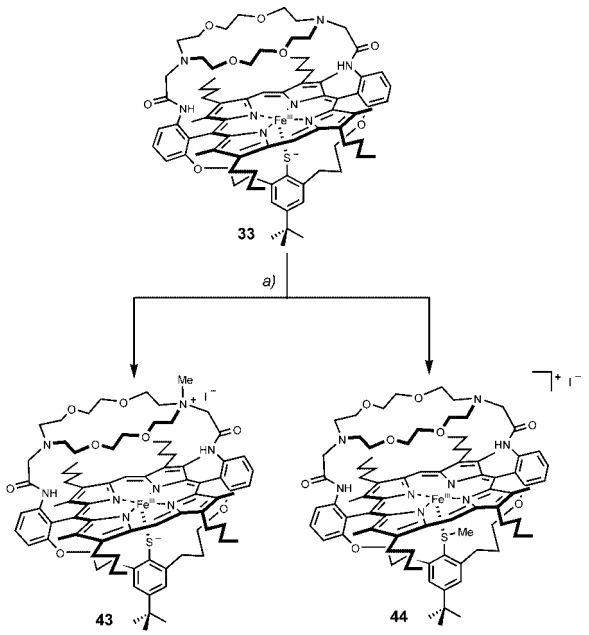

Scheme 12. Synthesis of *N*-alkylated crown-capped iron(III) porphyrin **43** and generation of *S*-alkylated side product **44**. *Reagents and conditions:* (a) MeI (291 equivs.) in portions over a time period of 20 h, toluene, rt, 24% **43** and 76% **44**.

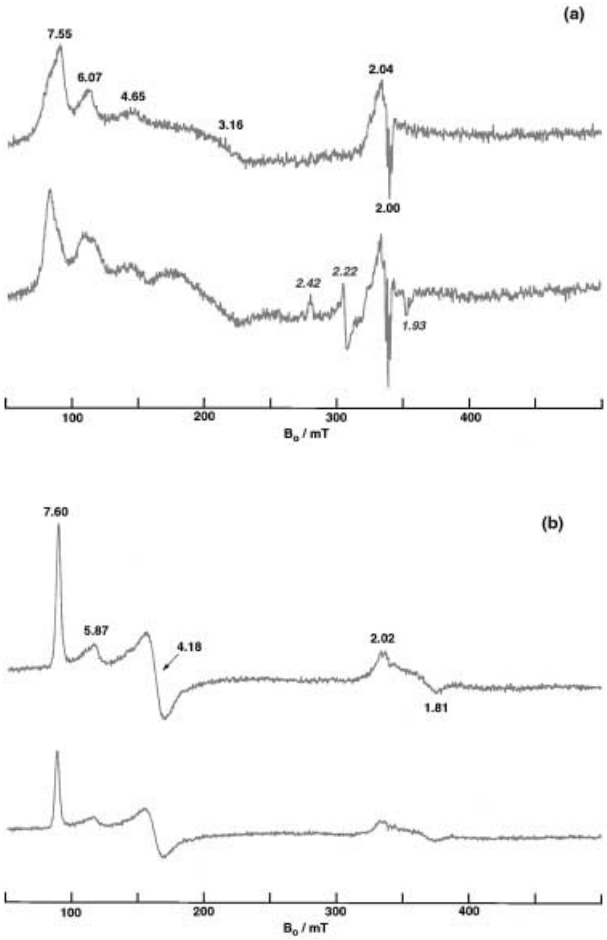

Figure 14. cw-EPR of *N*-methylated **43** (**a**) and *S*-methylated **44** (**b**) in dry toluene (top traces) and water-saturated toluene (bottom traces). Conditions: $\nu = 9.47$ GHz, $P = 20$ mW, $T =$ 100 K, modulation frequency 100 kHz, modulation amplitude 5.2 G.

by the idea of Collman et al.[33] who intended to synthesise water-soluble polyazacrown-capped porphyrins as oxygen carriers by alkylating the nitrogens of the polyazacrown caps, iron(III) porphyrin model compound **33** was reacted with an excess of iodomethane (Scheme 12). This yielded two products, both having the same mass according to ESI-MS and MALDI-TOF-MS but different colour, UV/Vis spectra and Rf values on TLC (Table 3).

Because of its brown colour, the very similar UV/Vis and cw-EPR spectra (*vide infra*) compared to the starting material **33** the less polar spot on TLC was assigned to the *N*-methylated compound **43**. Presumably, the more polar red compound which had a rather unusual UV/Vis and cw-EPR spectrum is *S*-methylated **44**. An *S*-methyl thiophenyliron(III) porphyrin was prepared in our group by Matile as a model compound for cytochrome *c*[34] and it displayed a *Soret* band at 424 nm. On the other hand, an *S*-methyl cytochrome *c* model compound synthesised by Nagano et al. showed a *Soret* band in the region of 415 nm.[35] Accordingly, the assignment of the red compound presented here may be inappropriate and **44** should be synthesised independently for comparison. However, it is also difficult to think of an alternative structure. Formation of a carbene species as observed with iron(II) porphyrins and $CDCl_3$ by Stäubli[27] seems rather unlikely.

As already mentioned the cw-EPR spectrum of brown product **43** in dry toluene was very similar to the

Table 3. Physical data of *N*- and *S*-methylated iron(III) porphyrins **43** and **44**.

Compound	Colour[a]	Rf[b]	UV/Vis[c] [nm (%)]	ESI-MS[d] [*m/z* (%)]
43	brown	0.58	404 (100); 513 (11)	1461 (100, M^+)
44	red	0.41	365 (sh, 58); 405 (100); 573 (18)	1461 (100, M^+)

[a] Toluene solution.
[b] Silica gel, toluene/THF, 2:1.
[c] In toluene at 298 K.
[d] In acetone.

spectrum of starting material **33** (Figure 14a, top trace) showing characteristic peaks for a rhombically distorted high-spin iron(III) species. However, when **43** was measured in water-saturated toluene the already known low-spin signals (Figure 14a, bottom trace) were observed to more or less the same extent as in the water complex **33**-H_2O and the Ba^{2+}/water complex **33**-H_2O/Ba^{2+} (*vide supra*).

The cw-EPR spectrum of the red compound **44** in dry toluene also shows signals for a pure rhombic high-spin iron(III) but with a completely different pattern (Figure 14b, top trace). Measuring the sample in water-saturated toluene results in an identical spectrum (Figure 14b, bottom trace). An interesting fact is that the spectra of **44** show a very high similarity with the high-spin portion of the cw-EPR spectrum of camphor-bound cytochrome $P450_{cam}$ (Figure 3).[7,8]

The results with the *N*-methylated crown-capped model **43** again point to the fact that a charge above the porphyrin plane does not influence the iron(III) spin state.

Conclusion

The water adducts of the crown-capped iron(III) thiolate porphyrins **33** and **34** proved to be active site analogues of the resting state of $P450_{cam}$. **33**-H_2O and **34**-H_2O, their corresponding Ba^{2+} complexes and **43**-H_2O are versatile model compounds to distinguish between two effects that could possibly modulate the spin state of heme-thiolate proteins (Figures 15 and 16).

Taking together the results presented in this work suggest that a distant charge above the porphyrin has no or very little effect on the spin state of the iron(III). Accordingly, the results do not support the predictions by Harris and Loew[17a] that the electrostatic field of the protein and the coordination of water modulate the spin

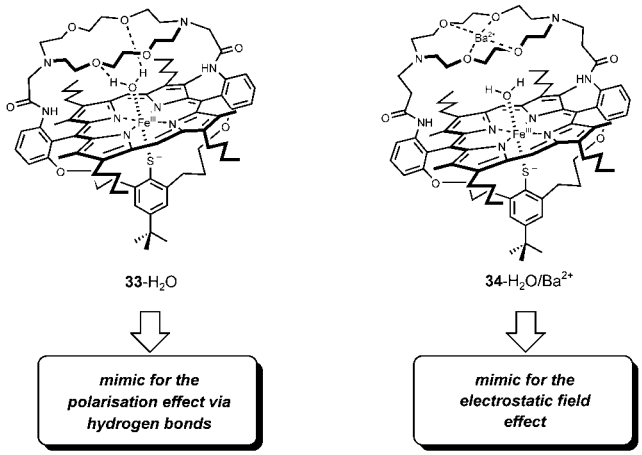

Figure 15. Separation of the remote charge and the polarisation effect by the model compounds **33**-H_2O and **34**-H_2O/Ba^{2+}.

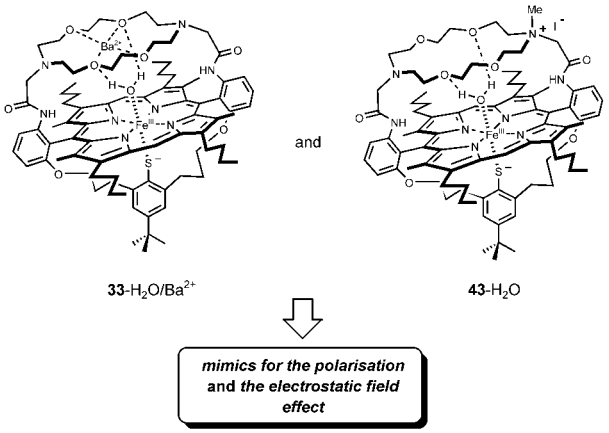

Figure 16. Model compounds for studying both effects simultaneously.

equilibrium of $P450_{cam}$. In contrast, it was qualitatively but clearly demonstrated that the spin equilibrium of the heme-thiolate cofactor shifts towards low-spin if the water coordinating to iron(III) adopts a distinctive hydroxide character due to hydrogen bonding interactions. This conclusion is also supported by calculations.[36]

In summary, experiments support that polarisation in the water cluster plays an important role for the observed low-spin resting state of $P450_{cam}$. Accordingly, the water coordinating to iron has a functional role[37] not only for adjusting E_o to -300 mV but also fine-tuning the spin state of the cofactor.

Experimental Section

General Remarks

Reagents were used as received from Fluka AG (Buchs, Switzerland), Merck AG (Darmstadt, Germany) and Aldrich (Buchs, Switzerland) unless otherwise stated. Chemicals of the quality *purum*, *purum p. a.* or >98% were used without further purification. 2,6-Lutidine for iron insertions was purchased from Aldrich, dried over solid KOH, distilled from BaO and degassed in high-vacuum by four freeze-pump-thaw cycles. Dry dichloromethane (CH_2Cl_2) was distilled from CaH_2, Et_2O and THF from Na/benzophenone, MeOH from Mg, DMF was dried over solid KOH and distilled from BaO, dioxane and toluene were distilled from Na. All freshly dried solvents were stored over activated molecular sieves. Further solvents used for reactions corresponded to the quality *puriss p. a., abs.,* over Molecular Sieves from Fluka AG. Degassed solvents for reactions under oxygen-free condition (e.g., in the glove box) were obtained by at least four freeze-pump-thaw cycles. For all non-aqueous reactions glassware was flame dried and the atmosphere was exchanged by argon. Iron insertions and all other reactions with iron porphyrins were carried out in a Labmaster 130 glove box (MBRAUN). The levels of dioxygen (<2 ppm) and water (<0.1 ppm) were measured with a

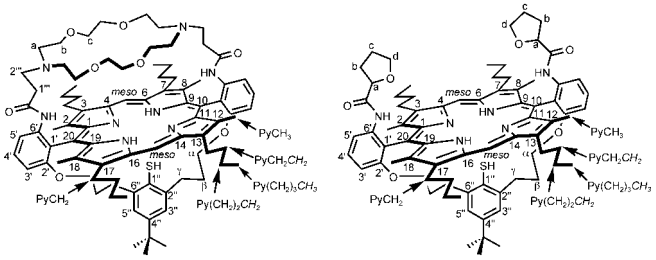

Figure 17. Atom numbering for NMR assignment.

combined H_2O/O_2-analyser (MBRAUN). All solvents and reagents used in the glove box were dried and degassed in high-vacuum. For flash chromatography silica gel 60 from Merck (0.043 – 0.06 mm, 230 – 400 mesh) or aluminium oxide 90 from Merck (standardised (activity II – III), 0.063 – 0.2 mm, 70 – 230 mesh) were used. Analytical RP-HPLC was performed on LiChrospher® 100 RP-18 silica gel from Merck (5 μm particle size, 4 × 250 mm column) with nanopure water and HPLC-grade MeOH or acetonitrile. Ultra violet-visible absorption spectra were recorded on a Hewlett-Packard 8452A Diode Array spectrophotometer and an Agilent 8453 Diode Array spectrophotometer. Infrared spectra were measured on a Perkin-Elmer 1600 series FTIR spectrometer in KBr (1% w/w). NMR was performed using either a Bruker av250 (250 MHz), Varian Gemini 300 (300 MHz), Bruker DPX-NMR (400 MHz), Bruker DRX-500 (500 MHz) or Bruker DRX-600 (600 MHz) spectrometer. $CDCl_3$ was filtered through basic alumina prior to use. δ_H and δ_C in ppm relative to residual solvent peaks. Porphyrin models atom numbering for NMR assignment see Figure 17.

EI-MS was measured on a Varian double focusing VG-70-250 spectrometer and ESI-MS were recorded on a Finnigan Mat LCQ-700. For MALDI-TOF-MS a Perseptive Biosystems Vestec Mass Spectrometry Products Voyager™ Elite Biospectrometry™ Research Station was used. cw-EPR was carried out using a Bruker ESP-300 X-band ($\nu_{microwave} = 9.485$ GHz) spectrometer equipped with a T_{102} cell and an ER4111VT liquid nitrogen cryostat to assure low temperature during measurement. Sample concentration was typically 5 mM and spectra were measured with a microwave power of 20 mW, modulation frequency of 100 kHz, and a modulation amplitude of 5.2 G.

tert-Butyl *N*-(2-Formyl-3-methoxyphenyl)carbamate (16)

tert-Butyl *N*-(3-methoxyphenyl)-carbamate (**19**) (4 g, 17.9 mmol) was dissolved in dry Et_2O (20 mL) and cooled to − 30 °C. To this solution was added dropwise a 1.5 M solution of *t*-BuLi (in hexane, 26.72 mL, 39.4 mmol) and the temperature was kept below − 15 °C. After having finished the addition the solution was stirred for 3 h at − 10 °C. Then the reaction mixture was cooled to − 78 °C and DMF (2.86 mL, 37.1 mmol) in dry Et_2O (5 mL) was added dropwise. Afterwards it was warmed to room temperature and stirring was continued overnight. The reaction was quenched with brine and extracted three times with Et_2O. The organic layers were separated, washed with water, dried over Na_2SO_4 and concentrated under vacuum. The viscous yellow oil was distilled bulb-to-bulb (180 °C/0.1 mbar) which gave the title compound as light yellow oil which solidified on standing at 4 °C; yield: 3.7 g (82%); Rf = 0.41 (hexane/ethyl acetate, 5:1). IR (KBr): ν = 3218 *m*, 3001 *m*, 2979 *m*, 2939 *m*, 2894 *m*, 1731 *s*, 1647 *s*, 1612 *s*, 1588 *s*, 1534 *s*, 1521 *s*, 1477 *s*, 1454 *s*, 1419 *s*, 1401 *s*, 1369 *s*, 1293 *s*, 1270 *s*,1229 *s*, 1199 *s*, 1157 *s*, 1049 *s*, 1027 *s*, 760 *m*, 718 *m* cm^{-1}; ^1H NMR (300 MHz, $CDCl_3$): δ = 10.96 (*br*, *s*, 1H, NH), 10.48 (*s*, 1H, CHO), 8.00 (*d*, *J* = 10.1 Hz, 1H, aryl H-5), 7.44 (*t*, *J* = 9.8 Hz, 1H, aryl H-4), 6.53 (*d*, *J* = 9.8, 1H, aryl H-3), 3.90 (*s*, 3H, OCH_3), 1.47 (*s*, 9H, *t*-Bu); EI-MS (70 eV): *m/z* (%) = 251 (14, M^+); 195 (25); 178 (25); 167 (16); 152 (5); 151 (44); 150 (7); 133 (6); 123 (15); 122 (43); 106 (6); 94 (9); 93 (16); 92 (5); 65 (7); 58 (6); 57 (100); 41 (27); 39 (9).

αα/αβ-10,20-Bis[6-(*tert*-butoxycarbonyl)amino-2-methoxyphenyl]-3,7,13,17-tetrabutyl-2,8,12,18-tetramethylporphyrin (αα/αβ-22)

A solution of *tert*-butyl *N*-(2-formyl-3-methoxyphenyl)carbamate (**16**) (4.59 g, 18.3 mmol) in MeCN (400 mL) was degassed by bubbling with argon for 15 min. Then 3,3′-dibutyl-4,4′-dimethyl-2,2′-dipyrrylmethane (**15**) (5.24 g, 18.3 mmol) was added with a spatula and the reaction mixture was bubbled with argon for another 15 min. After that *p*-toluenesulphonic acid (346 mg, 1.7 mmol) was added and the solution turned immediately dark-brown. Stirring was continued in the dark overnight at room temperature. For the subsequent oxidation of the formed porphyrinogens DDQ (8.29 g, 36.6 mmol) was dissolved in THF (80 mL) and added to the reaction mixture. The black mixture was stirred under air at room temperature and completion of the oxidation was followed with UV/Vis (CH_2Cl_2 + 1% Et_3N) by the disappearance of the porphyrinogen absorption at 483 nm and the appearance of the porphyrin *Soret* absorption at 406 nm. After 1.5 h all the volatiles were removed under vacuum which gave 20 g of crude product that was dissolved in CH_2Cl_2 and filtered through aluminium oxide. Fractions were controlled by TLC (silica gel, hexane/ethyl acetate, 3:1 + 1% Et_3N) and MALDI-TOF-MS and those displaying mass peaks at *m/z* = 1033 (M^+), 933 ([*M* – Boc]$^+$) and 833 ([*M* – 2 Boc]$^+$) were combined. After removing the solvent under reduced pressure this gave 5.26 g of porphyrin mixture as purple solid which was used without further purification for the next step.

αα/αβ-10,20-Bis(6-amino-2-methoxyphenyl)-3,7,13,17-tetrabutyl-2,8,12,18-tetramethylporphyrin (αα/αβ-23)

The porphyrin mixture (3.28 g, 3.17 mmol) from the previous step was dissolved in CH_2Cl_2 (300 mL) and a solution of trifluoroacetic acid (20 mL, 261 mmol) in CH_2Cl_2 (50 mL) was added within 20 min *via* a dropping funnel at room temperature. The greenish-purple solution was stirred for 12.5 h at room temperature. The reaction mixture was cooled in an ice bath and quenched with saturated aqueous $NaHCO_3$ (300 mL). After phase separation, the organic layer was washed again with saturated aqueous $NaHCO_3$ (200 mL). The combined aqueous phases were extracted with CH_2Cl_2 (2 × 100 mL) until colourless. The combined organic phases were finally washed with water (300 mL) and brine (200 mL), dried over Na_2SO_4 and concentrated under vacuum. The crude

product was purified by flash chromatography (silica gel, hexane/ethyl acetate, 6:1 + 1% Et_3N) which yielded 1.91 g (*72%*) of a 6:4-mixture of αα-**23** and αβ-**23**, respectively (estimated from ^1H NMR) as a purple solid. Rf = 0.34 (hexane/ethyl acetate, 3:1 + 1% Et_3N); UV/Vis (CH_2Cl_2 + 1% Et_3N): λ_{max} (%) = 410 (100, *Soret*), 508 (12), 542 (8), 574 (9), 586 nm (7). IR (KBr): ν = 3462 *m*, 3445 *m*, 3378 *m*, 2954 *s*, 2928 *s*, 2868 *s*, 2858 *s*, 1609 *s*, 1596 *s*, 1584 *s*, 1576 *s*, 1569 *s*, 1559 *m*, 1471 *s*, 1437 *s*, 1256 *s*, 1131 *s*, 1087 *s*, 762 *m* cm^{-1}; ^1H NMR (400 MHz, $CDCl_3$): δ = 10.16 (*s*, 2H, *meso*-H), 7.55 (*t*, *J* = 8.2 Hz, 2H, aryl H-4′), 6.76 (*m*, 4H, aryl H-3′, aryl H-5′), 4.00 (*m*, 8H, $PyCH_2$), 3.63 (*s*, 6H, αα-OCH_3), 3.55 (*s*, 6H, αβ-OCH_3), 3.36 (*br*, *s*, 2H, αβ-NH_2), 3.23 (*br*, *s*, 2H, αα-NH_2), 2.74 (*s*, 12H, $PyCH_3$), 2.17 (*m*, 8H, $PyCH_2CH_2$), 1.75 (*m*, 8H, $Py(CH_2)_2CH_2$), 1.09 (*t*, *J* = 7.3 Hz, 12H, $Py(CH_2)_3CH_3$), −2.32 (*br*, *s*, 2H, NH pyrrole); MALDI-TOF-MS: *m/z* (%) = 834 (100, $[M+1]^+$).

αα-10,20-Bis(6-acetylamino-2-methoxyphenyl)-3,7,13,17-tetrabutyl-2,8,12,18-tetramethyl-porphyrin (αα-24) and αβ-10,20-Bis(2-acetylamino-6-methoxyphenyl)-3,7,13,17-tetrabutyl-2,8,12,18-tetramethylporphyrin (αβ-24)

A solution of the atropisomeric mixture of porphyrin αα/αβ-**23** (1.91 g, 2.29 mmol) in dry CH_2Cl_2 (150 mL) was prepared and dry pyridine (0.4 mL, 7.64 mmol) and DMAP (60 mg, 0.49 mmol) added. Then a solution of acetyl chloride (0.4 mL, 5.63 mmol) in dry CH_2Cl_2 (75 mL) was added dropwise within 25 min at room temperature. The reaction mixture was stirred at room temperature for 18 h and quenched with saturated aqueous $NaHCO_3$ (150 mL) while cooling in an ice bath. The layers were separated and the aqueous phase was extracted with CH_2Cl_2 (2 × 75 mL). The combined organic layers were washed with water (250 mL) and brine (150 mL), dried over Na_2SO_4 and the solvents were evaporated under vacuum. Purification of the crude product and separation of the two atropisomers was achieved by repetitive flash chromatography (silica gel, hexane/ethyl acetate, 3:1 + 1% Et_3N, and hexane/ethyl acetate/CH_2Cl_2, 6:2:1 + 1% Et_3N). This yielded 1.02 g (49%) of αα-**24** and 512 mg (24%) of αβ-**24** as purple solids (combined yield: 73%).

Physical data of αα-**24**: Rf = 0.18 (hexane/ethyl acetate/CH_2Cl_2, 6:2:1 + 1% Et_3N); RP-HPLC (90–100% MeOH/H_2O in 25 min, then 100% MeOH for 5 min, flow 1.5 mL/min, λ_{det} = 410 nm, *T* = 40 °C): R_t = 12.2 min; UV/Vis (CH_2Cl_2 + 1% Et_3N): λ_{max} (%) = 410 (100, *Soret*), 508 (7), 542 (2), 574 (2), 628 nm (4); ^1H NMR (400 MHz, $CDCl_3$): δ = 10.26 (*s*, 2H, *meso*-H), 8.45 (*d*, *J* = 8.3 Hz, 2H, aryl H-5′), 7.81 (*t*, *J* = 8.5 Hz, 2H, aryl H-4′); 7.14 (*d*, *J* = 8.3 Hz, aryl H-3′), 6.51 (*br*, *s*, NHAc), 4.01 (*m*, 8H, $PyCH_2$), 3.60 (*s*, 6H, OCH_3), 2.61 (*s*, 12H, $PyCH_3$), 2.19 (*m*, 8H, $PyCH_2CH_2$), 1.75 (*m*, 8H, $Py(CH_2)_2CH_2$), 1.11 (*t*, *J* = 7.3 Hz, 12H, $Py(CH_2)_3CH_3$), 1.10 (*s*, 6H, $COCH_3$), −2.36 (*br*, *s*, 2H, NH pyrrole); MALDI-TOF-MS: *m/z* (%) = 917 (100, $[M+1]^+$), 939 (8, $[M+Na]^+$).

Physical data of αβ-**24**: Rf = 0.26 (hexane/ethyl acetate/CH_2Cl_2, 6:2:1 + 1% Et_3N); RP-HPLC (90–100% MeOH/H_2O in 25 min, then 100% MeOH for 5 min, flow 1.5 mL/min, λ_{det} = 410 nm, *T* = 40 °C): R_t = 10.6 min; UV/Vis (CH_2Cl_2 + 1% Et_3N): λ_{max} (%) = 410 (100, *Soret*), 508 (10), 542 (5), 574 (5), 588 nm (4); ^1H NMR (400 MHz, $CDCl_3$): δ = 10.25 (*s*, 2H, *meso*-H), 8.44 (*d*, *J* = 8.6 Hz, 2H, aryl H-5′), 7.81 (*t*, *J* = 8.5 Hz, 2H, aryl H-4′), 7.13 (*d*, *J* = 8.3 Hz, aryl H-3′), 6.49 (*br*, *s*, NHAc), 4.01 (*m*, 8H, $PyCH_2$), 3.57 (*s*, 6H, OCH_3), 2.60 (*s*, 12H, $PyCH_3$), 2.18 (*m*, 8H, $PyCH_2CH_2$), 1.73 (*m*, 8H, $Py(CH_2)_2CH_2$), 1.09 (*s*, 6H, $COCH_3$), 1.09 (*t*, *J* = 7.4 Hz, 12H, $Py(CH_2)_3CH_3$), −2.30 (*br*, *s*, 2H, NH pyrrole); MALDI-TOF-MS: *m/z* (%) = 917 (100, $[M+1]^+$), 939 (9, $[M+Na]^+$).

αα-10,20-Bis(6-acetylamino-2-hydroxyphenyl)-3,7,13,17-tetrabutyl-2,8,12,18-tetra-methylporphyrin (αα-25)

Porphyrin αα-**24** (1.03 g, 1.12 mmol) was dissolved in dry CH_2Cl_2 (75 mL) and to this solution was added ethanethiol (110 mL) followed by $AlCl_3$ (5.7 g, 42.7 mmol) in portions. The solution turned grass-green and it was stirred at room temperature for 43 h. The course of the reaction was followed by taking aliquots from the reaction mixture and injecting them into the RP-HPLC after a mini-work up [RP-HPLC: 90–100% MeCN/H_2O in 10 min, then 100% MeCN for 10 min, flow 1.5 mL/min, λ_{det} = 407 nm, *T* = 40 °C; R_t (product) = 4.4 min; R_t (monomethoxy side product) = 6.1 min; R_t (starting material) = 9.4 min]. The reaction was stopped by cooling the mixture in an ice bath and slow addition of saturated aqueous $NaHCO_3$ (200 mL). After separating the two phases the organic phase was washed with of saturated aqueous $NaHCO_3$ (2 × 140 mL). The aqueous phases were extracted with CH_2Cl_2 (2 × 200 mL) to minimise loss of material. The combined organic phases were washed with water (400 mL) and brine (300 mL), dried over Na_2SO_4 followed by removal of volatiles under vacuum. The crude amorphous purple solid was purified by flash chromatography (silica gel, hexane/ethyl acetate/CH_2Cl_2, 4:2:1 + 1% Et_3N) which yielded 726 mg (73%) of the title compound as purple solid; Rf = 0.34 (hexane/ethyl acetate, 1:1 + 1% Et_3N); RP-HPLC (90–100% MeCN/H_2O in 10 min, then 100% MeCN for 10 min, flow 1.5 mL/min, λ_{det} = 407 nm, *T* = 40 °C): R_t = 4.4 min; UV/Vis (CH_2Cl_2 + 1% Et_3N): λ_{max} (%) = 408 (100, *Soret*), 508 (8), 542 (4), 578 (4), 626 nm (2); IR (KBr): ν = 3530 *s*, 3403 *s*, 2955 *s*, 2928 *s*, 2859 *s*, 1676 *s*, 1588 *s*, 1527 *s*, 1466 *s*, 1370 *s*, 1339 *s*, 1273 *s*, 1178 *m*, 1156 *s*, 1138 *m*, 1100 *m*, 1038 *m*, 983 *m*, 950 *m*, 894 *w*, 846 *w*, 758 *m*, 735 *m*, 618 *m*, 576 *w* cm^{-1}; ^1H NMR (400 MHz, $CDCl_3$): δ = 10.34 (*s*, 2H, *meso*-H), 8.38 (*d*, *J* = 8.1 Hz, 2H, aryl H-5′), 7.75 (*t*, *J* = 8.3 Hz, 2H, aryl H-4′), 7.19 (*dd*, *J* = 8.3 Hz, *J* = 0.8 Hz, 2H, aryl H-3′), 6.44 (*s*, 2H, NHAc), 4.03 (*m*, 8H, $PyCH_2$), 2.69 (*s*, 12H, $PyCH_3$), 2.19 (*m*, 8H, $PyCH_2CH_2$), 1.77 (*m*, 8H, $Py(CH_2)_2CH_2$), 1.14 (*s*, 6H, CH_3CO), 1.11 (*t*, *J* = 7.5 Hz, 12H, $Py(CH_2)_3CH_3$), −2.31 (*br*, *s*, 2H, NH pyrrole); MALDI-TOF-MS: *m/z* (%) = 889 (100, $[M+1]^+$); 910 (12, $[M+Na]^+$).

Strapped porphyrin 27

To a solution of bisphenol porphyrin αα-**25** (6.9 mg, 7.8 μmol) in dry DMF (4 mL) was added Cs_2CO_3 (77 mg, 236 μmol, previously dried overnight at 100 °C in high vacuum). This suspension was heated to 60 °C and stirred for 30 min. Then a solution of 1,11-dibromoundecane (2.7 μL, 11 μmol) in dry DMF (1 mL) was added *via* a syringe pump within 3 h at 60 °C. Stirring was continued at 60 °C for 1 h after which the reaction mixture was poured into a ice-cooled mixture of 1 M HCl (2 mL) and CH_2Cl_2 (5 mL). The layers were separated and the

aqueous phase was extracted with CH_2Cl_2 (2×5 mL). The combined organic phases were washed with saturated aqueous $NaHCO_3$ (2×20 mL), water (10 mL) and brine (10 mL), dried over Na_2SO_4 and all volatiles were removed under vacuum. Purification by flash chromatography (silica gel, hexane/ethyl acetate, 2:1 + 1% Et_3N) yielded 5.1 mg (63%) of the title compound as purple solid; Rf = 0.56 (hexane/ethyl acetate, 1:1 + 1% Et_3N); UV/Vis (CH_2Cl_2 + 1% Et_3N): λ_{max} (%) = 410 (100, *Soret*), 508 (5), 542 (1), 580 (2), 628 nm (1); ^{1}H NMR (400 MHz, $CDCl_3$): δ = 10.23 (*s*, 2H, *meso*-H), 8.46 (*d*, *J* = 8.3 Hz, 2H, aryl H-5′), 7.77 (*t*, *J* = 8.3 Hz, 2H, aryl H-4′), 7.08 (*dd*, *J* = 8.3 Hz, *J* = 0.8 Hz, 2H, aryl H-3′), 6.86 (*s*, 2H, NHAc), 4.00 (*m*, 8H, $PyCH_2$), 3.82 (*m*, 4H, α-CH_2), 2.61 (*s*, 12H, $PyCH_3$), 2.20 (*m*, 8H, $PyCH_2CH_2$), 1.77 (*m*, 8H, $Py(CH_2)_2CH_2$), 1.21 (*s*, 6H, CH_3CO), 1.11 (*t*, *J* = 7.3 Hz, 12H, $Py(CH_2)_3CH_3$), 0.70 (*m*, 4H, β-CH_2), −0.34 (*m*, 4H, γ-CH_2), −0.67 (*m*, 4H, δ-CH_2), −1.61 (*br*, *s*, 6H, ε-CH2, ζ-CH2), −2.32 (*br*, *s*, 2H, NH pyrrole); MALDI-TOF-MS: *m/z* (%) = 1042 (100, $[M+1]^+$).

Thiocarbamoylbis(acetylamido)porphyrin 30

To a solution of bisphenol porphyrin αα-**25** (200 mg, 225 μmol) in dry DMF (90 mL) was added Cs_2CO_3 (2.21 g, 6.78 mmol) which was previously dried at 100 °C in high-vacuum overnight. The resulting suspension was heated to 60 °C and stirred for 30 min. Then a solution of dimesylate **17** (172 mg, 337 μmol) in dry DMF (28 mL) was added *via* a syringe pump within 4 h at 60 °C. Stirring was continued for 30 min at 60 °C after which the reaction mixture was cooled with an ice bath and the reaction was quenched with 1 M HCl (55 mL). For better phase separation CH_2Cl_2 (110 mL) was added. After phase separation the aqueous phase was extracted with CH_2Cl_2 (2×85 mL). The combined organic layers were washed with saturated aqueous $NaHCO_3$ (2×200 mL), water (170 mL) and brine (100 mL), dried over Na_2SO_4 and concentrated under reduced pressure. The crude product was purified by flash chromatography (silica gel, hexane/ethyl acetate, 2:1 + 1% Et_3N) which gave 230 mg (85%) of the bridged porphyrin as purple solid; Rf = 0.49 (hexane/ethyl acetate, 2:1 + 1% Et_3N); RP-HPLC (90–100% MeOH/H_2O in 10 min, then 100% MeOH for 10 min, flow 1.5 mL/min, λ_{det} = 414 nm, *T* = 40 °C): R_t = 10.3 min; UV/Vis (CH_2Cl_2 + 1% Et_3N): λ_{max} (%) = 414 (100, *Soret*), 511 (9), 543 (2), 578 (4), 632 nm (2); IR (KBr): ν = 3401 *m*, 2956 *s*, 2870 *s*, 1704 *s*, 1660 *s*, 1602 *s*, 1588 *s*, 1520 *s*, 1462 *s*. 1365 *m*, 1256 *s*, 1087 cm^{-1} *s*; ^{1}H NMR (400 MHz, $CDCl_3$): δ = 10.15 (*s*, 1H, *meso*-H), 9.72 (*s*, 1H, *meso*-H), 8.54 (*d*, *J* = 8.3 Hz, 2H, aryl H-5′), 7.79 (*s*, 2H, NHAc), 7.78 (*t*, *J* = 8.3 Hz, 2H, aryl H-4′), 6.97 (*d*, *J* = 8.3 Hz, 2H, aryl H-3′), 6.32 (*s*, 2H, aryl H-3″, aryl H-5″), 4.06 (*m*, 2H, $PyCH_2$), 3.99 (*m*, 2H, $PyCH_2$), 3.84 (*m*, 4H, $PyCH_2$ and α-CH_2), 3.61 (*m*, 4H, $PyCH_2$ and α-CH_2), 2.72 (*s*, 6H, $PyCH_3$), 2.54 (*s*, 6H, $PyCH_3$), 2.24 (*m*, 4H, $PyCH_2CH_2$), 1.94 (*m*, 2H, $PyCH_2CH_2$), 1.87 (*m*, 2H, $PyCH_2CH_2$), 1.79 (*m*, 4H, $Py(CH_2)_2CH_2$), 1.76 (*br*, *s*, NCH_3), 1.71 (*m*, 4H, $Py(CH_2)_2CH_2$), 1.54 (*s*, 6H, $COCH_3$), 1.15 (*t*, *J* = 7.3 Hz, 6H, $Py(CH_2)_3CH_3$), 1.13 (*t*, *J* = 7.3 Hz, 6H, $Py(CH_2)_3CH_3$), 1.06 (*s*, 9H, *t*-Bu), 0.59 (*m*, 6H, β-CH_2 and γ-CH_2), −0.04 (*m*, 2H, γ-CH_2), −1.17 (*br*, *s*, 3H, NCH_3), −2.13 (*br*, *s*, 2H, NH pyrrole); ^{13}C NMR (150 MHz, $CDCl_3$): δ = 168.8 (*s*, CO), 159.9 (*s*, aryl C-2′), 150.4 (*s*, aryl C-4″), 145.4 (*s*, C-12, C-18), 145.1 (*s*, C-2, C-8), 144.1 (*s*, aryl C-1″), 143.7 (*s*, C-3, C-7), 143.6 (*s*, C-13, C-17), 141.7 (*s*, C-14, C-16), 141.1 (*s*, C-4, C-6), 138.9 (*s*, C-1′), 135.9 (*s*, C-1, C-9), 135.5 (*s*, C-11, C-19), 130.8 (*d*, aryl CH-4′), 123.3 (*s*, aryl C-2″, aryl C-6″), 123.0 (*d*, aryl CH-3″, aryl CH-5″), 120.6 (*s*, aryl C-6′), 113.3 (*d*, aryl CH-5′), 109.3 (*d*, aryl CH-3′), 107.4 (*s*, C-10, C-20), 97.0 (*d*, *meso*-CH), 96.0 (*d*, *meso*-CH), 69.9 (*t*, α-CH_2), 35.6 (*t*, $PyCH_2CH_2$), 35.1 (*t*, $PyCH_2CH_2$), 34.0 (*s*, $C(CH_3)_3$), 32.5 (*q*, NCH_3), 31.0 (*q*, $C(CH_3)_3$), 30.6 (*t*, γ-CH_2), 28.6 (*t*, β-CH_2), 26.4 (*t*, $PyCH_2$), 26.1 (*t*, $PyCH_2$), 24.7 (*q*, $COCH_3$), 23.3 (*t*, $Py(CH_2)_2CH_2$), 23.2 (*t*, $Py(CH_2)_2CH_2$), 14.2 (*q*, $Py(CH_2)_3CH_3$), 14.1 (*q*, $Py(CH_2)_3CH_3$), 13.8 (*q*, $PyCH_3$), 13.4 (*q*, $PyCH_3$); MALDI-TOF-MS: *m/z* (%) = 1135 (11, $[M - CONMe_2]^+$); 1207 (100, $[M+1]^+$).

Thiocarbamoylbisaminoporphyrin 12

Bis(acetylamido)porphyrin **30** (222 mg, 184 μmol) was dissolved in MeOH (57 mL) and to this solution was added 6 M HCl (87 mL). The resulting grass-green solution was heated to reflux and stirred for 2 h after which the reaction mixture was cooled in an ice bath and the acid was neutralised dropwise with aqueous 50% NaOH (32 mL). The basic aqueous phase was extracted with CH_2Cl_2 (3×140 mL). The combined organic phases were washed with water (2×150 mL) and brine (140 mL), dried over Na_2SO_4 and all volatiles were removed under vacuum. After purification by flash chromatography (silica gel, hexane/ethyl acetate, 3:1 + 1% Et_3N) 188 mg (91%) of pure bisamino porphyrin **12** was obtained as purple solid; Rf = 0.66 (hexane/ethyl acetate, 1:1 + 1% Et_3N); RP-HPLC (90–100% MeOH/H_2O in 10 min, then 100% MeOH for 10 min, flow 1.5 mL/min, λ_{det} = 414 nm, *T* = 40 °C): R_t = 11.1 min (*broad*); UV/Vis (CH_2Cl_2 + 1% Et_3N): λ_{max} (%) = 414 (100, *Soret*), 510 (9), 544 (3), 578 (4), 631 nm (2); IR (KBr): ν = 3468 *w*, 3362 *m*, 2956 *s*, 2870 *m*, 1707 *w*, 1654 *s*, 1596 *s*, 1459 *s*, 1364 *m*, 1258 *s*, 1094 *m* cm^{-1}; ^{1}H NMR (400 MHz, $CDCl_3$): δ_H = 10.07 (*s*, 1H, *meso*-H), 9.65 (*s*, 1H, *meso*-H), 7.53 (*t*, *J* = 8.2 Hz, 2H, aryl H-4′), 6.87 (*d*, *J* = 8.3 Hz, 2H, aryl H-5′), 6.61 (*d*, *J* = 8.3 Hz, 2H, aryl H-3′), 6.32 (*s*, 2H, aryl H-3″, aryl H-5″), 4.29 (*br*, *s*, 4H, NH_2), 4.02 (*m*, 4H, $PyCH_2$), 3.88 (*m*, 2H, $PyCH_2$ and α-CH_2), 3.79 (*m*, 2H, $PyCH_2$ and α-CH_2), 3.57 (*m*, 4H, $PyCH_2$ and α-CH_2), 2.92 (*s*, 6H, $PyCH_3$), 2.69 (*s*, 6H, $PyCH_3$), 2.26 (*m*, 4H, $PyCH_2CH_2$), 1.95 (*m*, 2H, $PyCH_2CH_2$), 1.85 (*m*, 6H, $PyCH_2CH_2$ and $Py(CH_2)_2CH_2$), 1.79 (*br*, *s*, NCH_3), 1.71 (*m*, 4H, $Py(CH_2)_2CH_2$), 1.16 (*t*, *J* = 7.3 Hz, 6H, $Py(CH_2)_3CH_3$), 1.15 (*t*, *J* = 7.3 Hz, 6H, $Py(CH_2)_3CH_3$), 1.06 (*s*, 9H, *t*-Bu), 0.60 (*m*, 4H, β-CH_2), 0.48 (*m*, 2H, γ-CH_2), −0.04 (*m*, 2H, γ-CH_2), −1.16 (*br*, *s*, 3H, NCH_3), −2.07 (*br*, *s*, 2H, NH pyrrole); ^{13}C NMR (150 MHz, $CDCl_3$): δ = 167.1 (*s*, $CONMe_2$), 160.9 (*s*, aryl C-2′), 150.2 (*s*, aryl C-4″), 147.1 (*s*, aryl C-6′), 145.7 (*s*, C-12, C-18), 145.5 (*s*, C-2, C-8); 144.5 (*s*, arylC-1″); 142.9 (*s*, C-4, C-6, C-14, C-16); 141.3 (*s*, C-3, C-7); 140.9 (*s*, C-13, C-17), 136.1 (*s*, C-1, C-9), 135.6 (*s*, C-11, C-19), 130.3 (*d*, aryl CH-4′), 123.7 (*s*, aryl C-2″, aryl C-6″), 123.0 (*d*, aryl CH-3″, aryl CH-5″), 117.5 (*s*, aryl C-1′), 109.5 (*s*, C-10, C-20), 108.7 (*d*, aryl CH-5′), 103.9 (*d*, aryl CH-3′), 96.4 (*d*, *meso*-CH), 95.5 (*d*, *meso*-CH), 69.9 (*t*, α-CH_2), 35.8 (*t*, $PyCH_2CH_2$), 35.1 (*t*, $PyCH_2CH_2$), 34.0 (*s*, $C(CH_3)_3$), 32.2 (*q*, NCH_3), 31.1 (*q*, $C(CH_3)_3$), 31.08 (*t*, γ-CH_2), 28.8 (*t*, β-CH_2), 25.6 (*t*, $PyCH_2$), 26.2 (*t*, $PyCH_2$), 23.4 (*t*, $Py(CH_2)_2CH_2$), 14.3 (*q*, $Py(CH_2)_3CH_3$), 14.1 (*q*, $Py(CH_2)_3CH_3$), 13.4 (*q*, $PyCH_3$), 13.1 (*q*, $PyCH_3$); MALDI-TOF-MS: *m/z* (%) = 1052 (9, $[M + 1 - CONMe_2]^+$); 1123 (100, $[M+1]^+$).

Thiocarbamoylbis(THF)porphyrins *RR*,*SS*-31 and *RS*,*SR*-31

To a solution of bisaminoporphyrin **12** (117 mg, 104 μmol) in dry CH_2Cl_2 (22 mL) were added Et_3N (70 μL, 503 μmol) and DMAP (1.5 mg, 12 μmol). Then a solution of carbonyl chloride **13** (58 mg, 431 μmol) in dry CH_2Cl_2 (3 mL) was added dropwise at room temperature and the reaction mixture started to get cloudy ($Et_3N \cdot HCl$). Stirring was continued for 13 h after which the reaction mixture was cooled in an ice bath and the reaction was quenched with some pieces of ice and saturated aqueous $NaHCO_3$ (15 mL). After phase separation the organic layer was washed with saturated aqueous $NaHCO_3$ (2×20 mL) and water (20 mL). In order to reduce loss of material the aqueous phases were extracted with CH_2Cl_2 (2×10 mL). The combined organic phases were dried over Na_2SO_4 and concentrated under vacuum. The obtained residue was purified by flash chromatography (silica gel, hexane/ethyl acetate, 2:1 + 1% Et_3N) which yielded 97 mg (71%) of *RR*,*SS*-**31**, 17 mg (12%) of *RS*,*SR*-**31** and 12 mg (9%) of *RR*,*SS*/*RS*,*SR*-**31**, (92% combined yield) as purple solids. Actually, it is not necessary to separate the diastereoisomers since in the next step an epimerisation at a-CH of the tetrahydrofuranyl ring takes place.

Physical data of *RR*,*SS*-**31**: Rf = 0.37 (Et_2O); UV/Vis (CH_2Cl_2 + 1% Et_3N): λ_{max} (%) = 413 (100, *Soret*), 510 (9), 544 (4), 581 (4), 633 nm (2); ^{1}H NMR (400 MHz, $CDCl_3$): δ = 10.07 (*s*, 1H, *meso*-H), 9.66 (*s*, 1H, *meso*-H), 9.27 (*br*, *s*, 2H, NH amide), 8.55 (*d*, *J* = 8.6 Hz, 2H, aryl H-5′), 7.78 (*t*, *J* = 8.8 Hz, 2H, aryl H-4′), 6.98 (*d*, *J* = 7.3 Hz, 2H, aryl H-3′), 6.33 (*s*, 1H, aryl H-5″), 6.30 (*s*, 1H, aryl H-3″), 4.09 (*m*, 2H, a-CH), 4.00 (*m*, 4H, $PyCH_2$), 3.92 (*m*, 1H, $PyCH_2$), 3.85 (*m*, 2H, α-CH_2), 3.74 (*m*, 1H, $PyCH_2$), 3.58 (*m*, 4H, $PyCH_2$ and α-CH_2), 2.72 (*s*, 3H, $PyCH_3$), 2.67 (*s*, 3H, $PyCH_3$), 2.55 (*s*, 3H, $PyCH_3$), 2.49 (*s*, 3H, $PyCH_3$), 2.28 (*m*, 2H, d-CH_2), 2.23 (*m*, 4H, $PyCH_2CH_2$), 2.13 (*m*, 2H, b-CH_2), 1.96 (*m*, 1H, b-CH_2), 1.92 (*m*, 4H, $PyCH_2CH_2$), 1.82 (*m*, 4H, $Py(CH_2)_2CH_2$), 1.71 (*m*, 4H, $Py(CH_2)_2CH_2$), 1.68 (*m*, 1H, b-CH_2), 1.60 (*m*, 2H, d-CH_2), 1.17 (*m*, 12H, $Py(CH_2)_3CH_3$), 1.07 (*s*, 9H, *t*-Bu), 0.89 (*m*, 4H, c-CH_2), 0.60 (*m*, 6H, β-CH_2 and γ-CH_2), −0.05 (*m*, 2H, γ-CH_2), −1.07 (*br*, *s*, 3H, NCH_3), −1.98 (*br*, *s*, 2H, NH pyrrole); ^{13}C NMR (125 MHz, $CDCl_3$): δ = 172.2 (*s*, CO amide), 166.8 (*s*, CO thiocarbamate), 160.4, 160.0 (*s*, aryl C-2′), 150.4 (*s*, aryl C-4″·), 147.2 (*s*, C-12, C-18), 147.0 (*s*, C-2, C-8), 144.3 (*s*, C-13), 144.2 (*s*, C-17), 144.1 (*s*, C-3), 144.0 (*s*, C-7), 143.4 (*s*, C-14), 143.3 (*s*, C-16), 142.9 (*s*, C-4), 142.8 (*s*, C-6), 138.4 (*s*, arylC-6′), 136.0 (*s*, C-9), 135.6 (*s*, C-19), 135.2 (*s*, C-1), 134.9 (*s*, C-11), 130.8 (*d*, aryl CH-4′), 123.5 (*s*, aryl C-1″), 123.0 (*d*, aryl CH-3″, aryl CH-5″), 122.8 (*s*, aryl C-2″, aryl C-6″), 121.9, 121.2 (*s*, aryl C-1′); 113.2, 112.8 (*d*, aryl CH-5′); 110.3, 110.1 (*d*, aryl CH-3′), 107.5, 107.4 (*s*, C-10, C-20), 96.9, 96.1 (*d*, meso-CH), 78.4, 78.3 (*d*, a-CH), 69.7 (*t*, α-CH_2), 68.5, 68.3 (*t*, d-CH_2), 35.8, 35.2, 35.1 (*t*, $PyCH_2CH_2$), 34.1 (*s*, $C(CH_3)_3$), 31.6 (*q*, NCH_3), 31.1 (*q*, $C(CH_3)_3$), 30.8 (*t*, γ-CH_2), 30.3, 30.1 (*t*, b-CH_2), 28.8, 28.7 (*t*, β-CH_2), 26.6, 26.4, 26.1, 26.0 (*t*, $PyCH_2$), 24.2 (*t*, c-CH_2), 23.6, 23.5, 23.4, 23.3 (*t*, $Py(CH_2)_2CH_2$), 14.3, 14.1 (*q*, $Py(CH_2)_3CH_3$), 13.75, 13.63, 13.3, 13.2 (*q*, $PyCH_3$); MALDI-TOF-MS: *m*/*z* (%) = 1248 (5, $[M + 1 - CONMe_2]^+$); 1320 (100, $[M + 2]^+$).

Physical data of *RS*,*SR*-**31**: Rf = 0.31 (Et_2O); UV/Vis (CH_2Cl_2 + 1% Et_3N): λ_{max} (%) = 414 (100, *Soret*), 510 (10), 544 (5), 581 (5), 633 nm (1); ^{1}H NMR (400 MHz, $CDCl_3$): δ = 10.03 (*s*, 1H, *meso*-H), 9.71 (*s*, 1H, *meso*-H), 9.38 (*s*, 2H, NH amide), 8.63 (*d*, *J* = 8.6 Hz, 2H, aryl H-5′), 7.78 (*t*, *J* = 8.3 Hz, 2H, aryl H-4′), 6.96 (*d*, *J* = 8.3 Hz, 2H, aryl H-3′), 6.39 (*s*, 2H, aryl H-3″, aryl H-5″), 4.12 (*dd*, *J* = 8.6 Hz, *J* = 4.0 Hz, 2H, a-CH), 3.97 (*m*, 4H, $PyCH_2$), 3.91 (*m*, 2H, $PyCH_2$), 3.87 (*m*, 2H, α-CH_2), 3.59 (*m*, 4H, $PyCH_2$ and α-CH_2), 2.70 (*s*, 6H, $PyCH_3$), 2.54 (*s*, 6H, $PyCH_3$), 2.33 (*q*, *J* = 7.5 Hz, 2H, d-CH_2), 2.21 (*m*, 4H, $PyCH_2CH_2$), 2.15 (*m*, 2H, b-CH_2), 1.95 (*m*, 2H, b-CH_2), 1.85 (*m*, 8H, $PyCH_2CH_2$ and $Py(CH_2)_2CH_2$), 1.71 (*m*, 7H, $Py(CH_2)_2CH_2$ and NCH_3), 1.59 (*m*, 2H, d-CH_2), 1.42 (m, 4H, c-CH_2), 1.19 (*t*, *J* = 7.3, 6H, $Py(CH_2)_3CH_3$), 1.14 (*t*, *J* = 7.3, 6H, $Py(CH_2)_3CH_3$), 1.08 (*s*, 9H, *t*-Bu), 0.78 (*dt*, *J* = 3.5, *J* = 11.4, 2H, γ-CH_2), 0.66 (*m*, 2H, β-CH_2), 0.55 (*m*, 2H, β-CH_2), 0.13 (*dt*, *J* = 4.3, *J* = 13.1, 2H, γ-CH_2), −1.44 (*br*, *s*, 3H, NCH_3), −1.92 (*br*, *s*, 2H, NH pyrrole); ^{13}C NMR (125 MHz, $CDCl_3$): δ = 172.3 (*s*, CO amide), 160.0 (*s*, arylC-2′), 146.2 (*s*, C-12, C-18), 145.3 (*s*, C-2, C-8), 144.4 (*s*, arylC-4″), 143.8 (*s*, C-13, C-17), 143.6 (*s*, C-3, C-7), 143.4 (*s*, aryl C-1″), 140.9 (*s*, C-14, C-16), 140.4 (*s*, C-4, C-6), 138.4 (*s*, aryl C-1′), 135.6 (*s*, C-11, C-19), 135.1 (*s*, C-1, C-9), 131.0 (*d*, aryl CH-4′), 123.3 (*d*, aryl CH-3″, aryl CH-5″), 122.3 (*s*, aryl C-2″, aryl C-6”), 120.7 (*s*, aryl C-6′), 112.9 (*d*, aryl CH-5′), 109.2 (*d*, aryl CH-3′), 107.4 (*s*, C-10, C-20), 97.1, 95.8 (*d*, *meso*-CH), 78.3 (*d*, a-CH), 69.7 (*t*, α-CH_2), 68.4 (*t*, d-CH_2), 35.7, 35.1 (*t*, $PyCH_2CH_2$), 34.1 (*s*, $C(CH_3)_3$), 31.6 (*q*, NCH_3), 31.1 (*q*, $C(CH_3)_3$), 31.2 (*t*, γ-CH_2), 30.3 (*t*, b-CH_2), 28.9 (*t*, β-CH_2), 26.5, 26.1 (*t*, $PyCH_2$), 24.7 (*t*, c-CH_2), 23.6, 23.4 (*t*, $Py(CH_2)_2CH_2$), 14.2, 14.1 (*q*, $Py(CH_2)_3CH_3$), 13.7, 13.4 (*q*, $PyCH_3$); MALDI-TOF-MS: *m*/*z* (%) = 1249 (5, $[M + 2 - CONMe_2]^+$); 1320 (100, $[M + 2]^+$).

Bis(THF)thiophenolporphyrins *RR*,*SS*-32 and *RS*,*SR*-32

In a oxygen-free atmosphere thiocarbamoylporphyrin **31** (51 mg, 39 μmol) was dissolved in dry and degassed dioxane (10 mL) and the resulting solution was heated to 90 °C. Then a freshly prepared and degassed 2.18 M KOMe solution (in MeOH, 1 mL, 2.2 mmol) was added dropwise and the colour of the reaction mixture turned slightly green. The reaction mixture was heated to reflux and by blowing argon into the solution MeOH was evaporated until the solution was grass-green. Stirring at reflux was continued for 15 min after which the reaction was cooled in an ice bath and quenched with saturated aqueous NH_4Cl (6 mL). All of the used solvents and solutions for the aqueous work up were quickly degassed by bubbling with argon for 5–10 min prior to use. The obtained suspension was diluted with water (12 mL) and CH_2Cl_2 (20 mL). The layers were separated and the aqueous phase was extracted with CH_2Cl_2 (2×20 mL). The combined organic phases were washed with water (2×10 mL), dried over Na_2SO_4 and evaporated under reduced pressure. The crude product was purified by flash chromatography (silica gel, hexane/ethyl acetate, 3:1 + 1% Et_3N, under argon, solvents were quickly degassed by bubbling with argon for 15 min prior to use) and preparative TLC (silica gel, hexane/ethyl acetate, 3:1 + 1% Et_3N, under argon, solvents were quickly degassed by bubbling with argon for 15 min prior to use) which yielded 25.2 mg (52%) of *RR*,*SS*-**32** and 7.7 mg (16%) of *RS*,*SR*-**32** (combined yield: 68%) as purple solids.

Important note: the addition of 1% of Et_3N to the solvent system for chromatography is essential to achieve separation of the diastereoisomers.

Physical data for *RR*,*SS*-**32**: Rf = 0.29 (hexane/ethyl acetate, 2:1 + 1% Et_3N); UV/Vis (CH_2Cl_2 + 1% Et_3N): λ_{max} (%) = 412 (100, *Soret*), 510 (8), 545 (3), 577 (4), 632 nm (2); ^1H NMR (400 MHz, $CDCl_3$): δ = 10.13 (*s*, 2H, *meso*-H), 9.38 (*s*, 2H, NH amide), 8.65 (*d*, *J* = 7.9 Hz, 2H, aryl H-5′), 7.82 (*t*, *J* = 8.3, 2H, aryl H-4′), 7.01 (*d*, *J* = 7.7 Hz, 2H, aryl H-3′), 6.18 (*s*, 2H, aryl H-3″, aryl H-5″), 4.15 (*dd*, *J* = 8.5 Hz, *J* = 3.9 Hz, 2H, a-CH), 4.00 (*m*, 4H, $PyCH_2$), 3.91 (*m*, 4H, $PyCH_2$), 3.66 (*m*, 4H, α-CH_2), 2.66 (*s*, 6H, $PyCH_3$), 2.62 (*s*, 6H, $PyCH_3$), 2.26 (*m*, 2H, d-CH_2), 2.13 (*m*, 8H, $PyCH_2CH_2$), 2.10 (*m*, 2H, b-CH_2), 1.94 (*m*, 2H, b-CH_2), 1.77 (*m*, 8H, $Py(CH_2)_2CH_2$), 1.53 (*m*, 2H, d-CH_2), 1.23 (m, 4H, c-CH_2), 1.12 (*t*, *J* = 7.4, 12H, $Py(CH_2)_3CH_3$), 0.88 (*s*, 9H, *t*-Bu), 0.57 (*m*, 8H, β-CH_2 and γ-CH_2), −2.13 (*br*, *s*, 2H, NH pyrrole); −3.12 (*s*, 1H, SH); ^{13}C NMR (150 MHz, $CDCl_3$): δ = 172.3 (*s*, CO amide), 159.5 (*s*, aryl C-2′), 146.6 (*s*, C-2, C-8, C-12, C-18), 146.2 (*s*, aryl C-4″), 144.1 (*s*, C-14, C-16), 143.8 (*s*, C-4, C-6), 143.2 (*s*, C-13, C-17), 143.0 (*s*, C-3, C-7), 140.2 (*s*, C-10, C-20), 138.6 (*s*, aryl C-6′), 137.9 (*s*, aryl C-2″, aryl C-6″), 135.5 (*s*, C-11, C-19), 135.1 (*s*, C-1, C-9), 130.7 (*d*, aryl CH-4′), 126.5 (*s*, aryl C-1″), 122.9 (*d*, aryl C-3″, aryl C-5″), 121.5 (*s*, aryl C-1′), 113.1 (*d*, aryl CH-5′), 109.0 (*d*, aryl C-3′), 97.0 (*d*, *meso*-CH), 78.3 (*d*, a-CH), 68.5 (*t*, α-CH_2), 68.3 (*t*, d-CH_2), 35.6, 35.5 (*t*, $PyCH_2CH_2$), 33.6 (*s*, $C(CH_3)_3$), 30.9 (*q* and *t*, $C(CH_3)_3$ and γ-CH_2), 30.3 (*t*, b-CH_2), 28.9 (*t*, β-CH_2), 26.4, 26.5 (*t*, $PyCH_2$), 24.5 (*t*, c-CH_2), 23.4 (*t*, $Py(CH_2)_2CH_2$), 14.4 (*q*, $Py(CH_2)_2CH_3$), 13.5, 13.4 (*q*, $PyCH_3$); MALDI-TOF-MS: *m/z* (%) = 1248 (100, $[M+1]^+$).

Physical data for *RS*,*SR*-**32**: Rf = 0.24 (hexane/ethyl acetate, 2:1 + 1% Et_3N); UV/Vis (CH_2Cl_2 + 1% Et_3N): λ_{max} (%) = 413 (100, *Soret*), 510 (9), 544 (4), 577 (4), 631 nm (2); ^1H NMR (400 MHz, $CDCl_3$): δ = 10.12 (*s*, 1H, *meso*-H), 10.10 (*s*, 1H, *meso*-H), 9.41 (*s*, 2H, NH amide), 8.65 (*d*, *J* = 7.9 Hz, 2H, aryl H-5′), 7.81 (*t*, *J* = 8.3 Hz, 2H, aryl H-4′), 6.99 (*d*, *J* = 7.5 Hz, 2H, aryl H-3′), 6.21 (*s*, 2H, aryl H-3″, aryl H-5″), 4.16 (*dd*, *J* = 8.5 Hz, *J* = 4.2 Hz, 2H, a-CH), 3.95 (*m*, 8H, $PyCH_2$), 3.65 (*m*, 4H, α-CH_2), 2.64 (*s*, 12H, $PyCH_3$), 2.34 (*q*, *J* = 7.6 Hz, 2H, d-CH_2), 2.12 (*m*, 10H, $PyCH_2CH_2$ and b-CH_2), 1.96 (*m*, 2H, b-CH_2), 1.73 (*m*, 10H, $Py(CH_2)_2CH_2$ and d-CH_2), 1.26 (m, 4H, c-CH_2), 1.15 (*t*, *J* = 7.4 Hz, 6H, $Py(CH_2)_3CH_3$), 1.04 (*t*, *J* = 7.4, 6H, $Py(CH_2)_3CH_3$), 0.89 (*s*, 9H, *t*-Bu), 0.76 (*m*, 2H, γ-CH_2), 0.54 (*m*, 6H, β-CH_2 and γ-CH_2), −2.08 (*br*, *s*, 2H, NH pyrrole), −3.07 (*s*, 1H, SH); ^{13}C NMR (150 MHz, $CDCl_3$): δ = 172.3 (*s*, CO amide), 159.4 (*s*, aryl C-2′), 146.2 (*s*, aryl C-4″), 145.5 (*s*, C-12, C-18), 145.0 (*s*, C-2, C-8), 143.7 (*s*, C-14, C-16), 143.5 (*s*, C-4, C-6), 141.8 (*s*, C-10, C-20), 143.4 (*s*, C-3, C-7, C-13, C-17), 138.6 (*s*, aryl C-6′), 138.0 (*s*, aryl C-2″, aryl C-6″), 135.5 (*s*, C-11, C-19), 135.1 (*s*, C-1, C-9), 130.7 (*d*, aryl CH-4′), 126.4 (*s*, aryl C-1″), 123.1 (*d*, aryl C-3″, aryl C-5″), 121.2 (*s*, aryl C-1′), 113.0 (*d*, aryl CH-5′), 108.6 (*d*, aryl C-3′), 97.3, 96.6 (*d*, *meso*-CH), 78.3 (*d*, a-CH), 68.4 (*t*, d-CH_2), 67.1 (*t*, α-CH_2), 35.6, 35.5 (*t*, $PyCH_2CH_2$), 33.6 (*s*, $C(CH_3)_3$), 31.2 (*t*, γ-CH_2), 30.9 (*q*, $C(CH_3)_3$), 30.2 (*t*, b-CH_2), 29.0 (*t*, β-CH_2), 26.4 (*t*, $PyCH_2$), 24.5 (*t*, c-CH_2), 23.4, 23.3 (*t*, $Py(CH_2)_2CH_2$), 14.5 (*q*, $Py(CH_2)_2CH_3$), 13.5 (*q*, $PyCH_3$); MALDI-TOF-MS: *m/z* (%) = 1248 (100, $[M+1]^+$).

Thiocarbamoylbis(chloroacetylamido)porphyrin 36

In a experiment on a small scale bisaminoporphyrin **12** (4 mg, 3.6 μmol) was dissolved in dry CH_2Cl_2 (0.8 mL) and to this solution were added Et_3N (2.4 μL, 17.2 μmol) and one crystal of DMAP. Then a solution of freshly distilled chloroacetyl chloride (1.1 μL, 13.8 μmol) in dry CH_2Cl_2 (0.2 mL) was added dropwise *via* a syringe at room temperature. The reaction mixture was stirred at room temperature for 15 min after which it was cooled in an ice bath and the reaction was quenched with saturated aqueous $NaHCO_3$ (1 mL). The biphasic mixture was diluted with CH_2Cl_2 (2 mL), the phases were separated and the organic phase was washed with saturated aqueous $NaHCO_3$ (2 × 1 mL) and water (1 mL). In order to reduce loss of material the aqueous wash phases were extracted with CH_2Cl_2 (2 × 2 mL). The combined organic layers were dried over Na_2SO_4 and the solvent was evaporated under reduced pressure. The crude porphyrin was purified by preparative TLC (silica gel, hexane/ethyl acetate, 2:1 + 1% Et_3N) which yielded 2.8 mg (61%) of pure title compound as purple solid.

However, for the synthesis of larger amounts a reported procedure[30] was used: **12** (10.5 mg, 9.4 μmol) was dissolved in dry $CHCl_3$ (4 mL, filtered through basic aluminium oxide prior to use) and to this solution was added freshly distilled acetyl chloride (3 μL, 37.7 μmol) in dry $CHCl_3$ (0.4 mL). The resulting green solution was stirred at room temperature for 2.5 h after which the reaction was quenched with 0.1 M KOH (2 mL) in an ice bath. Furthermore, saturated aqueous $NaHCO_3$ (1 mL) and CH_2Cl_2 (2 mL) were added and the phases were separated. The organic layers were washed with water (5 mL) and brine (1 mL), dried over Na_2SO_4 and concentrated under vacuum. The obtained crude product (13 mg) was used without further purification for the next step. Rf = 0.31 (hexane/ethyl acetate, 2:1 + 1% Et_3N); RP-HPLC (90–100% MeOH/H_2O in 10 min, then 100% MeOH for 10 min, flow 1.5 mL/min, λ_{det} = 414 nm, *T* = 40 °C): R_t = 11.3 min.; UV/Vis (CH_2Cl_2 + 1% Et_3N): λ_{max} (%) = 413 (100, *Soret*), 510 (9), 544 (4), 579 (4), 633 nm (3); ^1H NMR (250 MHz, $CDCl_3$): δ = 10.15 (*s*, 1H, *meso*-H), 9.74 (*s*, 1H, *meso*-H), 9.09 (*s*, 2H, NH amide), 8.58 (*d*, *J* = 8.0 Hz, 2H, aryl H-5′), 7.83 (*t*, *J* = 8.3 Hz, 2H, aryl H-4′), 7.04 (*d*, *J* = 7.5 Hz, 2H, aryl H-3′), 6.38 (*s*, 2H, aryl H-3″, aryl H-5″), 4.09 (*m*, 2H, $PyCH_2$), 3.97 (*m*, 2H, $PyCH_2$), 3.88 (*m*, 4H, $PyCH_2$ and α-CH_2), 3.78 (*d*, *J* = 14.9 Hz, 2H, $COCH_2Cl$), 3.68 (*d*, *J* = 14.9 Hz, 2H, $COCH_2Cl$), 3.62 (*m*, 4H, $PyCH_2$ and α-CH_2), 2.74 (*s*, 6H, $PyCH_3$), 2.55 (*s*, 6H, $PyCH_3$), 2.26 (*m*, 4H, $PyCH_2CH_2$), 1.79 (*m*, 15H, $PyCH_2CH_2$, $Py(CH_2)_2CH_2$ and NCH_3), 1.17 (*t*, *J* = 7.3, 6H, $Py(CH_2)_3CH_3$), 1.16 (*t*, *J* = 7.2 Hz, 6H, $Py(CH_2)_3CH_3$), 1.10 (*s*, 9H, *t*-Bu), 0.68 (*m*, 6H, β-CH_2 and γ-CH_2), 0.06 (*m*, 2H, γ-CH_2), −1.17 (*br*, *s*, 3H, NCH_3), −1.97 (*br*, *s*, 2H, NH pyrrole); MALDI-TOF-MS: *m/z* (%) = 1206 (29, $[M+2-2\,Cl]^+$), 1242 (61, $[M+2-Cl]^+$), 1276 (100, $[M+2]^+$); ESI-MS (MeOH): *m/z* (%) = 1275 (20, $[M+H]^+$), 1297 (100, $[M+Na]^+$).

Crown-Capped Thiocarbamoylporphyrin 38

To a solution of bis(chloroacetylamido)porphyrin **36** (3 mg, 2.4 μmol) in dry EtOH (2.5 mL) was added 1,10-diaza-18-crown-6 (**35**) (3.1 mg, 11.8 μmol) in portions. The resulting red solution was heated to reflux and stirred for 21 h after which the reaction mixture was concentrated to dryness under reduced pressure. The crude residue was taken up in CH_2Cl_2 (4 mL) and washed with saturated aqueous $NaHCO_3$ (2 mL) and water (2 mL). In order to reduce loss of material the aqueous wash phases were extracted with CH_2Cl_2 (2 mL). The combined organic phases were dried over Na_2SO_4 and volatiles evaporated under vacuum. Purification by preparative TLC

(silica gel, CH_2Cl_2/MeOH, 95:5 + 1% Et_3N) yielded 2.4 mg (68%) of crown-capped porphyrin **38** as a purple varnish.

Alternatively, crude bis(chloroacetylamido)porphyrin **36** (11.8 mg, 9.25 μmol) (*vide supra*) was dissolved in dry EtOH (9.4 mL). To this solution was added 1,10-diaza-18-crown-6 (**35**) (12.3 mg, 46.9 μmol) in portions. The resulting reaction mixture was refluxed for 24 h and after analogous work-up and purification by flash chromatography (silica gel, CH_2Cl_2/MeOH 98:2) 7.6 mg (55% from **12**, 2 steps) of pure crown-capped porphyrin **38** were obtained. Rf = 0.51 (CH_2Cl_2/MeOH, 95:5 + 1% Et_3N); RP-HPLC (90–100% MeOH/H_2O in 10 min, then 100% MeOH for 10 min, flow 1.5 mL/min, λ_{det} = 414 nm, T = 40 °C): R_t = 11.5 min; UV/Vis (CH_2Cl_2 + 1% Et_3N): λ_{max} (%) = 414 (100, *Soret*), 510 (9), 542 (3), 578 (3), 632 nm (1); ^{1}H NMR (400 MHz, $CDCl_3$): δ = 10.19 (*s*, 1H, *meso*-H), 9.98 (*s*, 2H, NH amide), 9.64 (*s*, 1H, *meso*-H), 8.70 (*dd*, J = 7.9 Hz, J = 0.8 Hz, 2H, aryl H-5′), 7.79 (*t*, J = 8.3 Hz, 2H, aryl H-4′), 6.99 (*dd*, J = 8.0 Hz, J = 0.8 Hz, 2H, aryl H-3′), 6.29 (*s*, 2H, aryl H-3″, aryl H-5″), 3.98 (*m*, 4H, $PyCH_2$), 3.88 (*m*, 2H, $PyCH_2$ and α-CH_2), 3.79 (*m*, 2H, $PyCH_2$ and α-CH_2), 3.66 (*m*, 2H, $PyCH_2$ and α-CH_2), 3.59 (*m*, 2H, $PyCH_2$ and α-CH_2), 2.84 (*d*, J = 17.4, $COCH_2N$), 2.74 (*d*, J = 17.4, $COCH_2N$), 2.72 (*s*, 6H, $PyCH_3$), 2.53 (*s*, 6H, $PyCH_3$), 2.29 (*m*, 4H, $PyCH_2CH_2$), 2.03 (m, 4H, $PyCH_2CH_2$), 1.92 (*m*, 8H, $Py(CH_2)_2CH_2$ and c-CH_2), 1.75 (*m*, 11H, $Py(CH_2)_2CH_2$, c-CH_2 and NCH_3), 1.62 (*m*, 2H, b-CH_2), 1.33 (*m*, 2H, b-CH_2), 1.23 (*t*, J = 7.3, 6H, $Py(CH_2)_3CH_3$), 1.23 (*m*, 2H, b-CH_2), 1.19 (*t*, J = 7.5, 6H, $Py(CH_2)_3CH_3$), 1.14 (*m*, 2H, b-CH_2), 1.10 (*s*, 9H, *t*-Bu), 0.99 (*m*, 2H, a-CH_2), 0.62 (*m*, 4H, β-CH_2), 0.40 (*m*, 2H, γ-CH_2), 0.07 (*m*, 2H, a-CH_2), −0.14 (*m*, 2H, γ-CH_2), −0.28 (*m*, 2H, a-CH_2), −0.53 (*m*, 2H, a-CH_2), −0.68 (*br*, *s*, 3H, NCH_3), −2.12 (*s*, 2H, NH pyrrole); MALDI-TOF-MS: *m/z* (%) = 1395 (12, $[M + 2 - CONMe_2]^+$), 1466 (100, $[M + 2]^+$); ESI-MS (MeOH): positive ion mode: *m/z* (%) = 1487 (100, $[M + Na]^+$), 1503 (9, $[M + K]^+$); negative ion mode: *m/z* (%) = 1462 (100, $[M - H]^-$).

Crown-Capped Thiophenolporphyrin 40

In an oxygen-free atmosphere a solution of crown-capped porphyrin **38** (6.3 mg, 4.3 μmol) in dry and degassed dioxane (1.1 mL) was heated to 100 °C. To this hot solution was added a freshly prepared and degassed 2.18 M KOMe solution (in MeOH, 20 μL, 44 μmol) and the resulting grass-green solution was heated at reflux for 10 min. The reaction mixture was cooled in an ice bath and the reaction was quenched with saturated aqueous NH_4Cl (1 mL). All of the used solvents and solutions for the aqueous work up were quickly degassed by bubbling with argon for 5–10 min prior to use. For better phase separation the biphasic mixture was diluted with water (1 mL) and CH_2Cl_2 (2 mL). The aqueous layer was extracted with CH_2Cl_2 (2 × 2 mL), the combined organic layers were washed with water (3 mL), dried over Na_2SO_4 and concentrated under vacuum. The obtained crude residue was purified by preparative TLC (silica gel, CH_2Cl_2/MeOH, 95:5 + 1% Et_3N, under argon, solvents were quickly degassed by bubbling with argon for 5–10 min prior to use) which yielded 2.9 mg (48%) of pure thiophenolporphyrin **40**. It should be noted that it is essential to work under oxygen-free conditions and freshly prepared KOMe solution (instead of solid KOMe) should be used otherwise substantial amounts of *S*-oxidised products are generated and these are difficult to separate from the product. In the worst case arylsulphonic acid-porphyrin (SO_3H) **42** is the main product.

Physical data of thiophenol porphyrin **40**: Rf = 0.41 (CH_2Cl_2/MeOH 95:5 + 1% Et_3N); UV/Vis (CH_2Cl_2 + 1% Et_3N): λ_{max} (%) = 413 (100, *Soret*), 510 (9), 543 (4), 576 (4), 630 (2), 658 nm (1); ^{1}H NMR (250 MHz, $CDCl_3$): δ = 10.20 (*s*, 2H, *meso*-H), 10.05 (*s*, 2H, NH amide), 8.76 (*d*, J = 7.7 Hz, 2H, aryl H-5′), 7.82 (*t*, J = 8.4 Hz, 2H, aryl H-4′), 7.03 (*d*, J = 7.5 Hz, 2H, aryl H-3′), 6.13 (*s*, 2H, aryl H-3″, aryl H-5″), 3.98 (*m*, 8H, $PyCH_2$), 3.66 (*m*, 4H, α-CH_2), 2.84 (*s*, 4H, $COCH_2N$), 2.65 (*s*, 12H, $PyCH_3$), 2.22 (*m*, 8H, $PyCH_2CH_2$), 1.81 (*m*, 8H, $Py(CH_2)_2CH_2$), 1.76 (*m*, 8H, c-CH_2), 1.59 (*m*, 4H, b-CH_2), 1.44 (*m*, 4H, b-CH_2), 1.16 (*t*, J = 7.3, 12H, $Py(CH_2)_3CH_3$), 0.84 (*s*, 9H, *t*-Bu), 0.45 (*m*, 12H, β-CH_2, γ-CH_2 and a-CH_2), −0.17 (*m*, 4H, a-CH_2), −2.25 (*s*, 2H, NH pyrrole), −3.26 (*s*, 1H, SH); MALDI-TOF-MS: *m/z* (%) = 1395 (100, $[M + 2]^+$).

Physical data of *S*-oxidised (SO_3H) porphyrin **42**: Rf = 0.39 (CH_2Cl_2/MeOH, 95:5 + 1% Et_3N); UV/Vis (CH_2Cl_2 + 1% Et_3N): λ_{max} (%) = 412 (100, *Soret*), 508 (8), 542 (3), 577 (3), 632 nm (2); ^{1}H NMR (250 MHz, $CDCl_3$): δ = 10.50 (*s*, 2H, *meso*-H), 9.75 (*s*, 2H, NH amide), 8.73 (*d*, J = 8.2 Hz, 2H, aryl H-5′), 7.87 (*t*, J = 8.4 Hz, 2H, aryl H-4′), 7.11 (*d*, J = 7.9 Hz, 2H, aryl H-3′), 6.08 (*s*, 2H, aryl H-3″, aryl H-5″), 4.07 (*m*, 4H, $PyCH_2$), 3.98 (*m*, 4H, $PyCH_2$), 3.62 (*m*, 4H, α-CH_2), 2.81 (*s*, 4H, $COCH_2N$), 2.71 (*s*, 12H, $PyCH_3$), 2.24 (*m*, 8H, $PyCH_2CH_2$), 1.88 (*m*, 8H, $Py(CH_2)_2CH_2$), 1.74–1.57 (*m*, 16H, crown-CH_2), 1.22 (*t*, J = 7.4 Hz, 12H, $Py(CH_2)_3CH_3$), 0.88 (*s*, 9H, *t*-Bu), 0.57 (*m*, 4H, β-CH_2), 0.37 (*m*, 4H, γ-CH_2), 0.09 (*m*, 4H, crown-CH_2), −2.48 (*s*, 2H, NH pyrrole); MALDI-TOF-MS: *m/z* (%) = 1443 (100, $[M + 2]^+$), 1465 (15, $[M + 1 + Na]^+$), 1481 (6, $[M + 1 + K]^+$); ESI-MS (MeOH): positive ion mode: *m/z* (%) = 1442 (15, $[M + H]^+$), 1464 (100, $[M + Na]^+$), 1480 (17, $[M + K]^+$), 1486 (62, $[M - H + 2\ Na]^+$); negative ion mode: *m/z* (%) = 1440 (100, M^-).

Thiocarbamoylbis(acrylamido)porphyrin 37

Bisaminoporphyrin **12** (15 mg, 13.4 μmol) was dissolved in dry CH_2Cl_2 (2 mL) and to this solution was added Et_3N (50 μL, 359 μmol). Then a solution of freshly distilled acryloyl chloride (2.6 μL, 32 μmol) in dry CH_2Cl_2 (0.5 mL) was added dropwise *via* a syringe within 4 min at room temperature and stirring was continued for 4.5 h in the dark. The reaction mixture was cooled in an ice bath and saturated aqueous $NaHCO_3$ (2 mL) was added to quench the reaction. After phase separation the organic phase was washed with saturated aqueous $NaHCO_3$ (3 × 1 mL) and water (2 mL). To minimise loss of material the aqueous phases were extracted with CH_2Cl_2 (2 × 5 mL). The combined organic phases were dried over Na_2SO_4 and evaporated under reduced pressure. The obtained residue was purified by flash chromatography (silica gel, hexane/ethyl acetate, 2:1 + 1% Et_3N) which yielded 11.9 mg (72%) of the title compound as purple solid. It should be noted that this compound seems to be unstable, especially in solution, and therefore should be used as soon as possible for the next step. Rf = 0.28 (hexane/ethyl acetate, 2:1 + 1% Et_3N); RP-HPLC (90–100% MeOH/H_2O in 10 min, then 100% MeOH for 10 min, flow 1.5 mL/min, λ_{det} = 414 nm, T = 40 °C): R_t = 10.3 min; UV/Vis (CH_2Cl_2 + 1% Et_3N): λ_{max} (%) = 414 (100, *Soret*), 510 (6), 546 (2), 578 (1), 630 nm (1); ^{1}H NMR (400 MHz, $CDCl_3$): δ = 10.14 (*s*, 1H, *meso*-H), 9.72 (*s*, 1H,

meso-H), 8.68 (*d*, $J = 8.6$ Hz, 2H, aryl H-5′), 8.02 (*s*, 2H, NH amide), 7.80 (*t*, $J = 8.5$ Hz, 2H, aryl H-4′), 6.99 (*dd*, $J = 8.2$ Hz, $J = 0.6$ Hz, 2H, aryl H-3′), 6.33 (*s*, 2H, aryl H-3″, aryl H-5″), 5.84 (*dd*, $J_{trans} = 16.8$ Hz, $J = 0.9$ Hz, olefin H-2″$_{cis}$); 5.37 (*dd*, $J_{trans} = 16.9$ Hz, $J_{cis} = 10.4$ Hz, olefin H-1″), 5.13 (*dd*, $J_{cis} = 11.0$ Hz, $J = 0.8$ Hz, olefin H-2″$_{trans}$), 4.05 (*m*, 2H, $PyCH_2$), 3.98 (*m*, 2H, $PyCH_2$), 3.86 (*m*, 4H, $PyCH_2$ and α-CH_2), 3.61 (*m*, 4H, $PyCH_2$ and α-CH_2), 2.72 (*s*, 6H, $PyCH_3$), 2.55 (*s*, 6H, $PyCH_3$), 2.22 (*m*, 4H, $PyCH_2CH_2$), 1.94 (*m*, 2H, $PyCH_2CH_2$), 1.86 (*m*, 2H, $PyCH_2CH_2$), 1.77 (*m*, 4H, $Py(CH_2)_2CH_2$), 1.70 (*m*, 4H, $Py(CH_2)_2CH_2$), 1.14 (*t*, $J = 7.3$ Hz, 6H, $Py(CH_2)_3CH_3$), 1.11 (*t*, $J = 7.3$ Hz, 6H, $Py(CH_2)_3CH_3$), 1.07 (*s*, 9H, *t*-Bu), 0.59 (*m*, 6H, β-CH_2 and γ-CH_2), −0.02 (*m*, 2H, γ-CH_2), −1.02 (*br*, *s*, 3H, NCH_3), −2.14 (*br*, *s*, 2H, NH pyrrole); MALDI-TOF-MS: *m/z* (%) = 1160 (10, $[M + 1 - CONMe_2]^+$); 1231 (100, $[M + 1]^+$).

Crown-Capped Thiocarbamoylporphyrin 39

To a solution of bis(acrylamido)porphyrin **37** (167 mg, 136 μmol) in MeOH/CH_2Cl_2 25:1 (25 mL) was added 1,10-diaza-18-crown-6 (**35**) (180 mg, 686 μmol) in portions at room temperature. The resulting solution was heated at reflux for 44 h. The completion of the reaction was controlled by RP-HPLC (90–100% MeOH/H_2O in 10 min, then 100% MeOH for 10 min, flow 1.5 mL/min, $\lambda_{det} = 414$ nm, $T = 40\,^{\circ}C$; R_t (starting material) = 10.3 min, R_t (product) = 12.4 min). The reaction mixture was concentrated to dryness under vacuum and the crude product was purified by flash chromatography (aluminium oxide, CH_2Cl_2/MeOH, 100:1) which gave 133 mg (66%) of pure crown-capped porphyrin **39** as purple solid. Rf = 0.49 (aluminium oxide, CH_2Cl_2/MeOH, 100:1); RP-HPLC (90–100% MeOH/H_2O in 10 min, then 100% MeOH for 10 min, flow 1.5 mL/min, $\lambda_{det} = 414$ nm, $T = 40\,^{\circ}C$): R_t = 12.4 min; UV/Vis (CH_2Cl_2 + 1% Et_3N): λ_{max} (%) = 416 (100, *Soret*), 512 (6), 546 (1), 580 nm (1); ^1H NMR (400 MHz, $CDCl_3$): δ = 10.80 (*s*, 2H, NH amide), 10.15 (*s*, 1H, *meso*-H), 9.59 (*s*, 1H, *meso*-H), 8.70 (*d*, $J = 8.2$ Hz, 2H, aryl H-5′), 7.75 (*t*, $J = 8.3$ Hz, 2H, aryl H-4′), 6.94 (*d*, $J = 7.8$ Hz, 2H, aryl H-3′), 6.29 (*s*, 2H, aryl H-3″, aryl H-5″), 4.08 (*m*, 2H, $PyCH_2$), 3.90 (*m*, 2H, $PyCH_2$), 3.80 (*m*, 2H, α-CH_2), 3.74 (*m*, 2H, $PyCH_2$), 3.59 (*m*, 4H, $PyCH_2$ and α-CH_2), 2.75 (*s*, 6H, $PyCH_3$), 2.58 (*s*, 6H, $PyCH_3$), 2.28 (*m*, 4H, $PyCH_2CH_2$), 2.20 (*m*, 4H, 2‴-CH_2), 2.14 (*m*, 4H, c-CH_2), 2.03 (*m*, 4H, 1‴-CH_2), 1.95 (*m*, 8H, b-CH_2), 1.97 (*m*, 4H, $PyCH_2CH_2$), 1.91 (*sext*, $J = 7.2$ Hz, 4H, $Py(CH_2)_2CH_2$), 1.85 (*br*, *s*, 3H, NCH_3), 1.78 (*sext*, $J = 7.3$ Hz, 4H, $Py(CH_2)_2CH_2$), 1.21 (*t*, $J = 7.5$ Hz, 6H, $Py(CH_2)_3CH_3$), 1.19 (*t*, $J = 7.6$, 6H, $Py(CH_2)_3CH_3$), 1.14 (*m*, 4H, c-CH_2), 1.11 (*s*, 9H, *t*-Bu), 0.56 (*m*, 4H, β-CH_2), 0.39 (*dt*, $J = 4.4$ Hz, $J = 13.0$ Hz, 2H, γ-CH_2), 0.17 (*m*, 4H, a-CH_2), −0.08 (*m*, 4H, a-CH_2), −0.22 (*dt*, $J = 4.6$ Hz, $J = 13.2$ Hz, 2H, γ-CH_2), −0.69 (*br*, *s*, 3H, NCH_3), −2.09 (*br*, *s*, 2H, NH pyrrole); ^{13}C NMR (125 MHz, $CDCl_3$): $\delta_C = 172.1$ (*s*, CO amide), 166.6 (*s*, CO thiocarbamate), 160.5 (*s*, aryl C-2′), 150.4 (*s*, aryl C-4″), 146.1, 145.9 (*s*, C-1, C-9, C-11, C-19), 144.1 (*s*, aryl C-2″), 143.1, 141.7, 141.1 (*s*, C-4, C-6, C-14, C-16), 140.2 (*s*, aryl C-6′), 136.5, 135.9 (*s*, C-2, C-8, C-12, C-18), 130.9 (*d*, aryl CH-4′); 123.4 (*s*, arylC-1″), 122.5 (*d*, aryl CH-3″, aryl CH-5″), 121.2 (*s*, aryl C-1′), 114.2 (*d*, aryl CH-5′), 109.7 (*d*, aryl CH-3′), 109.2 (*s*, C-10, C-20), 96.7, 96.3 (*d*, *meso*-CH), 70.2, 70.0 (*t*, 1‴-CH_2), 68.2 (*t*, b-CH_2), 65.2 (*t*, c-CH_2), 49.3 (*t*, a-CH_2), 47.5 (*t*, 2‴-CH_2), 36.2, 35.5 (*t*, $PyCH_2CH_2$), 34.1 (*s*, $C(CH_3)_3$), 33.9 (*t*, α-CH_2), 31.2 (*q*, $C(CH_3)_3$), 26.6, 26.1 (*t*, $PyCH_2$), 24.5 (*t*, $Py(CH_2)_2CH_2$), 14.1 (*q*, $Py(CH_2)_3CH_3$), 13.8, 13.4 (*q*, $PyCH_3$); MALDI-TOF-MS: *m/z* (%) = 1494 (100, $[M + 1]^+$), 1531 (12, $[M + K]^+$).

Crown-Capped Thiophenolporphyrin 41

In an oxygen-free atmosphere thiocarbamoylporphyrin **39** (126 mg, 85 μmol) was dissolved in dry and degassed dioxane (15 mL). The resulting solution was heated at 100 °C and then a freshly prepared and degassed 1.8 M KOMe solution (in MeOH, 0.48 mL, 860 μmol) was added *via* a syringe. The colour of the reaction mixture turned immediately grass-green and it was heated at reflux for 10 min. The reaction mixture was cooled with an ice bath and the reaction was quenched with saturated aqueous NH_4Cl (6 mL). All of the used solvents and solutions for the aqueous work-up were quickly degassed by bubbling with argon for 5–10 min prior to use. The layers were separated and the aqueous phase was extracted with CH_2Cl_2 (2 × 50 mL). The combined organic phases were washed with water (2 × 50 mL), dried over Na_2SO_4 and concentrated under vacuum. Purification of the residue by flash chromatography (silica gel, CH_2Cl_2/MeOH, 97:3, under argon, solvents were quickly degassed by bubbling with argon for 15 min prior to use) yielded 98 mg (81%) of crown-capped thiophenolporphyrin **41** as purple solid. Rf = 0.54 (silica gel, CH_2Cl_2/MeOH, 95:5); UV/Vis (CH_2Cl_2 + 1% Et_3N): λ_{max} (%) = 415 (100, *Soret*), 510 (7), 544 (2), 576 (3), 630 nm (1); ^1H NMR (400 MHz, $CDCl_3$): δ = 10.89 (*s*, 2H, NH amide), 10.12 (*s*, 2H, *meso*-H), 8.74 (*dd*, $J = 8.2$ Hz, $J = 0.8$ Hz, 2H, aryl H-5′), 7.75 (*t*, $J = 8.5$ Hz, 2H, aryl H-4′), 6.93 (*dd*, $J = 8.1$ Hz, $J = 0.8$ Hz, 2H, aryl H-3′), 6.10 (*s*, 2H, aryl H-3″, aryl H-5″), 3.98 (*m*, 4H, $PyCH_2$), 3.90 (*m*, 4H, $PyCH_2$), 3.80 (*t*, $J = 4.7$ Hz, 4H, α-CH_2), 2.65 (*s*, 12H, $PyCH_3$), 2.21 (*q*, $J = 5.5$ Hz, 4H, 2‴-CH_2), 2.17 (*m*, 8H, $PyCH_2CH_2$), 2.05 (*t*, $J = 5.6$ Hz, 4H, 1‴-CH_2), 1.98 (*m*, 8H, c-CH_2), 1.82 (*sext*, $J = 7.0$ Hz, 8H, $Py(CH_2)_2CH_2$), 1.12 (*t*, $J = 7.3$ Hz, 6H, $Py(CH_2)_3CH_3$), 1.04 (*m*, 8H, b-CH_2), 0.82 (*s*, 9H, *t*-Bu), 0.41 (*m*, 4H, γ-CH_2), 0.34 (*m*, 4H, β-CH_2), 0.10 (*t*, $J = 5.4$ Hz, 8H, a-CH_2), −2.27 (*br*, *s*, 2H, NH pyrrole), −3.33 (*s*, 1H, SH); ^{13}C NMR (125 MHz, $CDCl_3$): δ = 172.1 (*s*, CO amide), 159.7 (*s*, aryl C-2′), 146.2 (*s*, aryl C-4″), 145.9 (*s*, C-1, C-9, C-11, C-19), 143.2 (*s*, C-3, C-7, C-13, C-17), 141.6 (*s*, C-4, C-6, C-14, C-16), 140.3 (*s*, aryl C-6′), 137.8 (s, aryl C-2″, aryl C-6″), 136.0 (*s*, C-2, C-8, C-12, C-18), 130.5 (*d*, aryl CH-4′), 126.5 (*s*, aryl C-1″), 123.0 (*d*, aryl CH-3″, aryl CH-5″), 121.2 (*s*, aryl C-1′), 114.2 (*d*, aryl CH-5′), 109.2 (*s*, C-10, C-20), 108.3 (*d*, aryl CH-3′), 96.9 (*d*, *meso*-CH), 68.5 (*t*, α-CH_2), 68.3 (*t*, b-CH_2), 65.3 (*t*, c-CH_2), 49.3 (*t*, a-CH_2), 47.5 (*t*, 2‴-CH_2), 36.0 (*t*, $PyCH_2CH_2$), 33.9 (*t*, 1‴-CH_2), 33.6 (*s*, $C(CH_3)_3$), 31.0 (*t*, γ-CH_2), 30.1 (*q*, $C(CH_3)_3$), 29.0 (*t*, β-CH_2), 26.5 (*t*, $PyCH_2$), 23.5 (t, $Py(CH_2)_2CH_2$), 14.3 (*q*, $Py(CH_2)_3CH_3$), 13.6 (*q*, $PyCH_3$); MALDI-TOF-MS: *m/z* (%) = 1422 (100, $[M + 1]^+$); ESI-MS (MeOH/H_2O, 10:1 + 0.1% NH_3): *m/z* (%) = 1422 (100, $[M + H]^+$).

Bis(THF)iron Porphyrins *RR*,*SS*/*RS*,*SR*-11 and *RR*,*SS*-11

To a solution of thiophenolporphyrin *RR*,*SS*/*RS*,*SR*-**32** (11.8 mg, 9.5 μmol) in dry and degassed toluene (3.5 mL) was added dry and degassed 2,6-lutidine (19 μL, 164 μmol) and the

resulting red solution was heated to reflux. Then a suspension of $FeBr_2$ (17.9 mg, 83 μmol) in dry and degassed toluene (0.5 mL) was added and the dark brown reaction mixture was stirred at reflux for 1 h. After cooling to room temperature the reaction mixture was filtered through a small pad of celite and the residue was washed with small toluene portions until the filtrate was colourless. The combined brown filtrates were concentrated under vacuum and the obtained residue was purified by column chromatography (silica gel, hexane/ethyl acetate, 2:1) which gave 11.4 mg (92%) of iron porphyrin *RR*,*SS*/*RS*,*SR*-**11** as a brown solid.

The same experiment was carried out with the pure diastereoisomer *RR*,*SS*-**32** (7 mg, 5.6 μmol). Treatment with dry and degassed 2,6-lutidine (13 μL, 112 μmol) and $FeBr_2$ (12 mg, 55.6 μmol) yielded 5.9 mg (79%) of iron porphyrin *RR*,*SS*-**11** as a brown solid after work-up and purification. Rf = 0.16 (hexane/ethyl acetate, 2:1); UV/Vis (toluene): λ_{max} (%) = 404 (100, *Soret*), 517 nm (12); MALDI-TOF-MS: *m/z* (%) = 1301 (100, $[M+1]^+$), 1324 (11, $[M+1+Na]^+$); ESI-MS (MeOH): positive ion mode: *m/z* (%) = 1301 (6, $[M+H]^+$), 1323 (100, $[M+Na]^+$); negative ion mode: *m/z* (%) = 1300 (100, M^-); cw-EPR (toluene, T = 100 K): g = 8.33, 5.32, 3.08, 2.08, 2.00 (rhombic, high-spin).

Crown-Capped Iron Porphyrin 33

As for **11** thiophenolporphyrin **40** (2.9 mg, 2.1 μmol) was treated with dry and degassed 2,6-lutidine (5 μL, 43 μmol) and $FeBr_2$ (5.4 mg, 25 μmol) in dry and degassed toluene at reflux for 30 min. Work-up and purification by column chromatography (silica gel, conditioned with toluene, eluted with toluene/THF, 3:1) yielded 2.8 mg (92%) of iron porphyrin **33** as a brown solid. Rf = 0.39 (toluene/THF, 3:1); UV/Vis (toluene): λ_{max} (%) = 404 (100, *Soret*), 517 (12), 644 nm (5); MALDI-TOF-MS: *m/z* (%) = 1447 (100, $[M+2]^+$), 1469 (29, $[M+Na]^+$); ESI-MS (MeOH): *m/z* (%) = 1469 (100, $[M+Na]^+$); cw-EPR (toluene, T = 100 K): g = 8.20, 6.00, 4.82, 3.38, 2.04, 2.01 (rhombic, high-spin).

Crown-Capped Iron Porphyrin 34

Analogously, thiophenolporphyrin **41** (10.9 mg, 7.7 μmol) was reacted with dry and degassed 2,6-lutidine (17 μL, 71 μmol) and $FeBr_2$ (15.2 mg, 71 μmol) in dry and degassed toluene at reflux for 30 min. Work-up and purification by column chromatography (silica gel, conditioned with toluene, eluted with toluene/THF 1:1) furnished 5 mg (44%) of iron porphyrin **34** as a brown solid. Important note: if this reaction is carried out on a larger scale (> 10 mg of **41**) or if applying prolonged reaction periods the yield drops drastically (decomposition). Rf = 0.48 (toluene/THF, 1:1); UV/Vis (toluene): λ_{max} (%) = 406 (100, *Soret*), 516 nm (11); MALDI-TOF-MS: *m/z* (%) = 1475 (100, $[M+1]^+$), 1498 (19, $[M+1+Na]^+$); ESI-MS (MeOH): *m/z* (%) = 1497 (100, $[M+Na]^+$); 1513 (5, $[M+K]^+$); cw-EPR (toluene, T = 100 K): g = 8.39, 7.50, 5.47, 4.91, 3.15, 2.47, 2.04, 2.00 (rhombic, high-spin).

Generation of Iron(III) Porphyrin Water Complexes; General Procedure

A biphasic mixture of degassed toluene and degassed water (2:1 v/v) was stirred vigorously for 30 min at room temperature. Stirring was stopped and phase separation awaited. The upper organic phase was used for dissolving the iron porphyrins, such that 5 mM solutions in wet toluene were obtained. These solutions were used directly for cw-EPR measurements. cw-EPR (water-saturated toluene, T = 100 K): Data for **33**-H_2O: g = 8.20, 6.00, 4.82, 3.38, 2.04, 2.01 (rhombic, high-spin); 2.42, 2.22, 1.93 (rhombic, low-spin). Data for **34**-H_2O: g = 8.20, 6.00, 4.82, 3.38, 2.04, 2.01 (rhombic, high-spin). Data for *RR*,*SS*-**11**-H_2O: g = 8.26, 5.17, 3.08, 2.03, 2.00 (rhombic, high-spin); 2.22, 2.15, 1.97 (rhombic, low-spin).

Bis(THF)iron Porphyrin Imidazole Complex *RR*,*SS*/*RS*,*SR*-11-Im

Iron porphyrin *RR*,*SS*/*RS*,*SR*-**11** (3 mg, 2.3 μmol) was dissolved in a dry and degassed 0.2 M imidazole solution (in DMF, 1 mL, 200 μmol) and the resulting brown solution was stirred at room temperature for 20 h. The reaction mixture was used directly for analysis. Note: judging from cw-EPR the imidazole complex *RR*,*SS*/*RS*,*SR*-**11**-Im is not stable during column chromatography. UV/Vis (toluene): λ_{max} (%) = 404 (100, *Soret*);, 520 nm (11); MALDI-TOF-MS: *m/z* (%) = 1301 (100, $[M+1-ImH]^+$); ESI-MS (MeOH): *m/z* (%) = 1301 (36, $[M+H-ImH]^+$), 1323 (100, $[M+Na-ImH]^+$); cw-EPR (DMF, T = 104 K): g = 2.42, 2.21, 1.92 (rhombic, low-spin).

Crown-Capped Iron Porphyrin Imidazole Complex 34-Im

Similarly, crown-capped iron porphyrin **34** (3 mg, 2 μmol) in a dry and degassed 0.2 M imidazole solution (in DMF, 1 mL, 200 μmol) was stirred at room temperature for 39 h. The resulting reaction mixture was use for analysis directly. Note: the imidazole complex is not stable during column chromatography. UV/Vis (toluene): λ_{max} (%) = 406 (100, *Soret*), 517 nm (8); MALDI-TOF-MS: *m/z* (%) = 1475 (82, $[M+1-ImH]^+$), 1497 (100, $[M+Na-ImH]^+$), 1514 (16, $[M+1+K-ImH]^+$); ESI-MS (MeOH): *m/z* (%) = 1475 (10, $[M+H-ImH]^+$), 1497 (100, $[M+Na-ImH]^+$), 1513 (7, $[M+K-ImH]^+$); cw-EPR (DMF, T = 104 K): g = 8.25, 5.20, 3.20, 2.08, 2.00 (rhombic, high-spin); 2.45, 2.21, 1.91 (rhombic, low-spin).

Barium Crown Ether Complexes; General Procedure

To 1 equivalent of crown-capped iron porphyrin were added 5 equivalents of $Ba(ClO_4)_2$ as a dry and degassed 4 mM solution (in acetone). The resulting mixture was treated with ultrasound for 5 min at room temperature after which it was used directly for the analysis. In order to study the influence of the counteranion the mixture of crown-capped iron porphyrin **33** and $Ba(ClO_4)_2$ in acetone was evaporated to dryness under reduced pressure. The obtained residue was dissolved in a dry and degassed 7 mM *n*-Bu_3N(TRISPHAT) solution (in CH_2Cl_2, 2 equivalents) and for reasons of solubility dry and degassed acetone was added also. The resulting mixture was stirred at

room temperature for 2 h after which it was used directly for the analysis.

Data for **33**-H_2O/Ba^{2+}: ESI-MS (acetone): *m/z* (%) = 792 (83, $[M + Ba]^{2+}$), 1447 (100, $[M + H]^+$), 1469 (19, $[M + Na]^+$), 1683 (11, $[M + Ba + ClO_4]^+$); cw-EPR (water-saturated toluene, $T = 100$ K): g = 8.20, 6.00, 4.78, 3.39, 2.04, 2.00 (rhombic, high-spin); 2.42, 2.21, 1.92 (rhombic, low-spin).

Data for (**33**-H_2O/Ba^{2+})[TRISPHAT]: ESI-MS (acetone): positive ion mode: *m/z* (%) = 186 (100, $[Bu_3NH]^+$), 724 (25, $[M + 2\,H]^{2+}$), 792 (34, $[M + Ba]^{2+}$), 1447 (30, $[M + H]^+$), 1683 (16, $[M + Ba + ClO_4]^+$); negative ion mode: *m/z* (%) = 769 (100, $[TRISPHAT]^-$); cw-EPR (water-saturated toluene, $T = 100$ K): g = 8.08, 5.80, 4.69, 3.45, 2.03, 2.00 (rhombic, high-spin); 2.21 (rhombic, low-spin).

Data for **34**-Ba^{2+}: ESI-MS (acetone): *m/z* (%) = 738 (9, $[M + 2\,H]^{2+}$), 806 (37, $[M + Ba]^{2+}$), 1475 (50, $[M + H]^+$), 1497 (100, $[M + Na]^+$), 1711 (90, $[M + Ba + ClO_4]^+$); cw-EPR (acetone, $T = 100$ K): g = 8.26, 5.47, 3.25, 2.75, 2.03, 2.00 (rhombic, high-spin).

N-Methylated Crown-Capped Iron Porphyrin (43)

Crown-capped iron porphyrin **33** (1.2 mg, 0.83 μmol) was dissolved in dry and degassed toluene (200 μL) and to this solution was added MeI (15 μL, 240 μmol) in portions over a time period of 20 h while stirring at room temperature. The course of the reaction was followed ESI-MS. The reaction mixture was concentrated to dryness under vacuum and the brown residue was purified by column chromatography (silica gel, conditioned with toluene, eluted with toluene/THF, 5:1). This yielded 0.4 mg (24%) of *N*-methylated crown-capped iron porphyrin **43** as a brown microcrystalline powder and 1.3 mg of a red compound which is presumably the *S*-methylated iron porphyrin **44**.

Physical data of *N*-methylated crown-capped **43**: Rf = 0.58 (toluene/THF, 2:1); UV/Vis (toluene): λ_{max} (%) = 404 (100, *Soret*), 513 nm (11); ESI-MS (acetone): *m/z* (%) = 1446 (37, $[M - CH_3]^+$), 1461 (100, M^+); MALDI-TOF-MS: *m/z* (%) = 1447 (100, $[M + 1 - CH_3]^+$), 1461 (86, M^+), 1470 (27, $[M + 1 + Na - CH_3]^+$), 1485 (13, $[M + K - CH_3]^+$); cw-EPR (toluene, $T = 100$ K): g = 7.55, 6.07, 4.65, 3.16, 2.04, 2.00 (rhombic, high-spin); cw-EPR (water-saturated toluene, $T = 100$ K): g = 8.20, 6.07, 4.71, 3.34, 2.04, 2.00 (rhombic, high-spin); 2.42, 2.22, 1.93 (rhombic, low-spin).

Physical data of red compound **44**: Rf = 0.41 (toluene/THF, 2:1); UV/Vis (toluene): λ_{max} (%) = 365 (*sh*, 58), 405 (100, *Soret*), 573 nm (18); ESI-MS (acetone): *m/z* = 1461 (100, M^+), 1501 (64); MALDI-TOF-MS: *m/z* = 1461 (100, M^+); cw-EPR (toluene, $T = 100$ K): g = 7.60, 5.87, 4.18, 2.02, 1.81 (rhombic, high-spin); cw-EPR (water-saturated toluene, $T = 100$ K): g = 7.66, 5.84, 4.18, 2.03, 1.81 (rhombic, high-spin).

Acknowledgements

Financial support from the Swiss National Science Foundation is gratefully acknowledged.

References and Notes

[1] W.-D. Woggon, *Top. Curr. Chem.* **1996**, *184*, 40.
[2] P. R. Ortiz de Montellano, in *Cytochrome P450: Structure, Mechanism, and Biochemistry*, (Ed.: P. R. Ortiz de Montellano), 2nd edn., Plenum Press, New York, **1995**.
[3] F. Durst, in *Frontiers in Biotransformation*, (Eds.: K. Ruckpaul, H. Rein), Akademie Verlag, Berlin, **1991**, p. 191.
[4] F. P. Guengerich, in *Mammalian cytochrome P450,* Vol. 1–2, CRC, Boca Raton, Florida, **1987**.
[5] a) T. L. Poulos, B. C. Finzel, A. J. Howard, *Biochemistry* **1986**, *25*, 5314; b) T. L. Poulos, B. C. Finzel, A. J. Howard, *J. Mol. Biol.* **1987**, *195*, 687; c) R. Raag, T. L. Poulos, *Biochemistry* **1991**, *30*, 2674; d) R. Raag, T. L. Poulos, *Biochemistry* **1989**, *28*, 7586; e) H. Li, S. Narasimhulu, L. M. Havran, J. D. Winkler, T. L. Poulos, *J. Am. Chem. Soc.* **1995**, *117*, 6297.
[6] I. Schlichting, J. Berendzen, K. Chu, A. M. Stock, S. A. Maves, D. E. Benson, R. M. Sweet, D. Ringe, G. A. Petsko, S. G. Sligar, *Science* **2000**, *287*, 1615.
[7] S. G. Sligar, *Biochemistry* **1976**, *15*, 5399.
[8] R. Tsai, C. A. Yu, I. C. Gunsalus, J. Peisach, W. E. Blumberg, W. H. Orme-Johnson, H. Beinert, *Proc. Nat. Acad. Sci. USA* **1970**, *66*, 1157.
[9] M. Sharrock, E. Münck, P. G. Debrunner, V. Marshall, J. D. Lipscomb, I. C. Gunsalus, *Biochemistry* **1973**, *12*, 258.
[10] S. G. Sligar, I. C. Gunsalus, *Proc. Nat. Acad. Sci. USA* **1976**, *73*, 1078.
[11] J. T. Groves, *J. Chem. Educ.* **1985**, *62*, 928.
[12] H. B. Dunford, J. S. Stillman, *Coord. Chem. Rev.* **1976**, *19*, 187.
[13] a) S. P. de Visser, F. Ogliaro, P. K. Sharma, S. Shaik, *Angew. Chem. Int. Ed.* **2002**, *41*, 1947; b) F. Ogliaro, S. Cohen, M. Filatov, N. Harris, S. Shaik, *Angew. Chem. Int. Ed.* **2000**, *39*, 3851; c) F. Ogliaro, S. P. de Visser, J. T. Groves, S. Shaik, *Angew. Chem. Int. Ed.* **2001**, *40*, 2874; d) S. P. de Visser, F. Ogliaro, P. K. Sharma, S. Shaik, *J. Am. Chem. Soc.* **2002**, *124*, 11809.
[14] a) S. Shaik, M. Filatov, D. Schröder, H. Schwarz, *Chem. Eur. J.* **1998**, *4*, 193; b) D. Schröder, S. Shaik, H. Schwarz, *Acc. Chem. Res.* **2000**, *33*, 139.
[15] R. Raag, T. L. Poulos, in *Frontiers in Biotransformation,* (Eds.: K. Ruckpaul, H. Rein), Vol. 7, Akademie Verlag, Berlin, **1992**, p. 1.
[16] a) D. Goldfarb, M. Bernardo, H. Thomann, P. M. H. Kroneck, V. Ullrich, *J. Am. Chem. Soc.* **1996**, *118*, 2686; b) H. Thomann, M. Bernardo, D. Goldfarb, P. M. H. Kroneck, V. Ullrich, *J. Am. Chem. Soc.* **1995**, *117*, 8243.
[17] a) D. Harris, G. Loew, *J. Am. Chem. Soc.* **1993**, *115*, 8775; b) D. Harris, G. Loew, *personal communication*.
[18] a) H. Aissaouï, S. Ghirlanda, C. Gmür, W.-D. Woggon, *J. Mol. Catal. A* **1996**, *113*, 393; b) H. Aissaouï, R. Bachmann, A. Schweiger, W.-D. Woggon, *Angew. Chem.* **1998**, *110*, 3191.
[19] E. Alonso, C. del Pozo, J. Gonzalez, *J. Chem. Soc. Perkin Trans. 1* **2002**, 571–576.

[20] Y. Kondo, S. Kojima, T. Sakamoto, *J. Org. Chem*. **1997**, *62*, 6507 – 6511.
[21] P. Stanetty, H. Koller, M. Mikovilovic, *J. Org. Chem.* **1992**, *57*, 6833.
[22] P. S. Clesy, G. A. Smythe, *Aust. J. Chem.* **1969**, *22*, 239.
[23] A. Osuka, B. Liu, K. Marayama, *J. Org. Chem.* **1993**, *58*, 3582.
[24] X.-X. Zhang, S. J. Lippard, *J. Org. Chem.* **2000**, *65*, 5298.
[25] B. Stäubli, H. Fretz, U. Piantini, W.-D. Woggon, *Helv. Chim. Acta* **1987**, *70*, 1173.
[26] W.-D. Woggon, H.-A. Wagenknecht, C. Claude, *J. Inorg. Biochem.* **2001**, *83*, 289.
[27] B. Stäubli, *PhD thesis*, University of Zürich (Switzerland), **1989**.
[28] R. Boss, A. I. Popov, *Inorg. Chem.* **1986**, *25*, 1747.
[29] C. Comte, C. P. Gros, S. Koeller, R. Guilard, D. J. Nurco, K. M. Smith, *New J. Chem.* **1998**, 621.
[30] a) J. P. Collman, X. Zhang, P. C. Herrmann, E. S. Uffelman, B. Boitrel, A. Straumanis, J. I. Brauman, *J. Am. Chem. Soc.* **1994**, *116*, 2681; b) J. P. Collman, P. C. Herrmann, L. Fu, T. A. Eberspacher, M. Eubanks, B. Boitrel, P. Hayoz, X. Zhang, J. I. Brauman, V. W. Day, *J. Am. Chem. Soc.* **1997**, *119*, 3481.
[31] J. Lacour, S. Torche-Haldimann, J. J. Jodry, C. Ginglinger, F. Favarger, *Chem. Commun.* **1998**, 1733.
[32] This material was kindly provided by Prof. J. Lacour.
[33] X. Zhang, E. S. Uffelman, J. P. Collman, (Univ. of Stanford), *US Patent* 5,384,397, **1995**; *Chem. Abstr.* **1995**, *123*, 143544.
[34] S. Matile, W.-D. Woggon, *J. Chem. Soc. Chem. Commun.* **1990**, 774.
[35] T. Dokoh, N. Suzuki, T. Higuchi, Y. Urano, K. Kikuchi, T. Nagano, *J. Inorg. Biochem.* **2000**, *82*, 127.
[36] M. Lochner, M. Meuwly, W.-D. Woggon, *J. Chem. Soc. Chem. Commun.* **2003**, in print.
[37] E. Meyer, *Protein Science* **1992**, *1*, 1543.

